OAK RIDGE NATIONAL LABORATORY LIBRARIES

3 4456 0551583 1

ORNL/TM-6673

Analytical Investigation of the Applicability of an Isochronous Method for Predicting Creep Deformations in Structures at Elevated Temperatures

J. A. Clinard

4-0727

This document does not contain UCNI, ECI, or other unclassified sensitive information and has been approved for release to the public by:

David R. Hamrin 11/10/2010
David R. Hamrin, ORNL Classification Officer Date

[redacted]

OAK RIDGE NATIONAL LABORATORY
CENTRAL RESEARCH LIBRARY
CIRCULATION SECTION
4500N ROOM 175
LIBRARY LOAN COPY
DO NOT TRANSFER TO ANOTHER PERSON
If you wish someone else to see this report, send in name with report and the library will arrange a loan.

OAK RIDGE NATIONAL LABORATORY
OPERATED BY UNION CARBIDE CORPORATION · FOR THE DEPARTMENT OF ENERGY

Printed in the United States of America. Available from
the Department of Energy,
Technical Information Center
P.O. Box 62, Oak Ridge, Tennessee 37830
Price: Printed Copy $5.25 ; Microfiche $3.00

This report was prepared as an account of work sponsored by an agency of the United States Government. Neither the United States Government nor any agency thereof, nor any of their employees, contractors, subcontractors, or their employees, makes any warranty, express or implied, nor assumes any legal liability or responsibility for any third party's use or the results of such use of any information, apparatus, product or process disclosed in this report, nor represents that its use by such third party would not infringe privately owned rights.

ORNL/TM-6673
Dist. Category UC-79,
-79h, -79k

Contract No. W-7405-eng-26

Engineering Technology Division

ANALYTICAL INVESTIGATION OF THE APPLICABILITY OF AN ISOCHRONOUS METHOD FOR PREDICTING CREEP DEFORMATIONS IN STRUCTURES AT ELEVATED TEMPERATURES

J. A. Clinard

Date Published - June 1979

Prepared by the
OAK RIDGE NATIONAL LABORATORY
Oak Ridge, Tennessee 37830
operated by
UNION CARBIDE CORPORATION
for the
DEPARTMENT OF ENERGY

OAK RIDGE NATIONAL LABORATORY LIBRARIES

3 4456 0551583 1

CONTENTS

	Page
HIGHLIGHTS	1
1. INTRODUCTION	2
2. BEAM AND PLATE PROBLEMS	4
2.1 Test of Beam B9	4
2.2 Test of Plate CP5	6
3. MATERIAL BEHAVIOR DESCRIPTIONS	9
3.1 Material Descriptions for Detailed Inelastic Analyses	9
3.2 Material Descriptions for Isochronous Stress-Strain Analyses	10
4. DETAILED SOLUTIONS	14
4.1 Detailed Solution of Beam B9	14
4.2 Detailed Solution of Plate CP5	20
5. ISOCHRONOUS SOLUTIONS	25
5.1 Isochronous Stress-Strain Solution of Beam B9	25
5.2 Isochronous Stress-Strain Solution of Plate CP5	25
6. COMPARISON OF SOLUTIONS	34
6.1 Comparison of Solutions to Test Data	34
6.2 Comparisons Between the Solutions	37
7. SUMMARY AND RECOMMENDATIONS	42
8. ACKNOWLEDGMENTS	45
9. REFERENCES	46
Appendix. USE OF ISOCHRONOUS STRESS-STRAIN METHODS IN PIPING ANALYSIS	47

ANALYTICAL INVESTIGATION OF THE APPLICABILITY OF AN ISOCHRONOUS METHOD FOR PREDICTING CREEP DEFORMATIONS IN STRUCTURES AT ELEVATED TEMPERATURES*

J. A. Clinard

HIGHLIGHTS

This report presents results for a limited analytical investigation of the applicability of an isochronous stress-strain method for predicting creep deformations in structures at elevated temperatures.

Two demonstration problems were selected from available benchmark experimental tests conducted at Oak Ridge National Laboratory (ORNL) to help assess the predictive capabilities of the method. The problems considered were a rectangular beam and a circular plate, both of which were simply supported and centrally loaded. Only monotonic loadings were investigated; these produced significant plastic and creep deformations.

The two problems were analyzed using both the detailed elastic-plastic-creep method currently recommended for design analysis of high-temperature reactor components and the isochronous method which is a simplification of the detailed method. The isochronous solutions were compared to experimental results and to the detailed solutions, and observations concerning the agreement were made.

It was found that the isochronous solutions were cheaper than the detailed solutions by an appreciable amount. Also, the isochronous predictions, though they included effects of creep in a qualitatively correct fashion, varied considerably with data and with the detailed predictions. The agreement was better for the beam than for the plate.

The study supports the proposition of using the isochronous stress-strain method as a simplified design method to account for creep in structures. However, it is believed that theoretical consistency of the method must be demonstrated and that guidelines for implementation in design practice must be developed and set forth.

Keywords: isochronous, detailed inelastic analysis, simplified inelastic analysis, type 304 stainless steel, high-temperature structural design, structural tests, beam, plate, finite-element, isothermal, plasticity, creep.

---

*Work performed under DOE/RRT 189a OH048, High-Temperature Structural Design.

1. INTRODUCTION

The elevated-temperature operating conditions of fast breeder reactors have led to the development of rational design and analysis procedures which account for inelastic structural behavior. A methodology for design of breeder structures which combines data, state-of-the-art inelastic constitutive theories, and analytical methods is given in Ref. 1. Incidences may arise in design practice which necessitate invoking the methodology to the extent of performing detailed multidimensional inelastic analyses for the purpose of design assessment or, in some cases, for satisfaction of various ASME Code criteria.[2] Because of the great expense and time required in performing detailed analyses, much work has been directed toward the development of simplified methods which are more practical for use in design iterations and which may, in fact, reduce the incidences of required detailed analysis.

Most of these simplified methods involve a relaxation of strict mechanistic principles, either through geometric or material simplifications or both. One method for material simplification is the so-called "isochronous stress-strain method" which approximately determines the monotonic creep response from a related elastic-plastic analysis. The procedure followed is to develop the isochronous curve for the desired time, and to employ this curve as short-time uniaxial stress-strain data for a time-independent elastic-plastic analysis, thus estimating the structural response due to creep at a savings compared to a detailed time-dependent analysis.

The isochronous method addressed in this study should not be confused with the isochronous techniques currently included in Appendix T of Ref. 2. Reference 2 offers guidelines for the use of isochronous stress-strain curves in <u>elastic</u> methods for the determination of creep-ratchetting strain (in T-1324, Test No. 3, the O'Donnell-Porowski method) and for the evaluation of fatigue damage (in T-1432). The method investigated in this study is an <u>inelastic</u> method which indirectly estimates deformations due to creep through time-independent structural analysis.

Many questions concerning the validity and usefulness of inelastic isochronous methods have not been satisfactorily answered. The effects

of the gross simplifications of the constitutive equations have not been fully appraised; furthermore, the method has not been developed to the degree necessary for general applicability (indeed, at present only certain monotonic loadings may be treated), and guidelines for implementation in design practice have not been set forth. These questions and needs are currently being addressed in the Westinghouse High-Temperature Structural Design-Application Program (WARD 189a CW138) (see Ref. 3) as part of the DOE/RRT effort to establish a suitable high-temperature structural design technology for breeder reactors. Work reported herein was performed independently of but in support of WARD activities.

This report investigates the predictive capabilities of the isochronous method through demonstrative analyses of benchmark tests performed at ORNL and reported in Ref. 4. Comparisons are made among isochronous solutions, detailed elastic-plastic-creep solutions, and actual test data for one beam and one plate test. Both structures were of type 304 stainless steel with isothermal test conditions of 593°C (1100°F). In each of the two check cases only a single constant-load creep period was considered.

Three specific questions are partially answered:

1. What accuracy may be assigned to isochronous stress-strain predictions?
2. How closely do isochronous predictions match detailed inelastic predictions?
3. What cost savings may be realized through the utilization of this simplified method?

The following two chapters describe the ORNL beam and plate tests analyzed in this study and detail the material models employed in the analyses. Next, three chapters are included which present the detailed inelastic and isochronous solutions and make comparisons among the solutions and actual test data. The last chapter summarizes current activities and offers recommendations for future work. The appendix attempts to bring into focus another related activity concerned with the use of the isochronous stress-strain method in simplified piping analysis.

2. BEAM AND PLATE PROBLEMS

Two problems were selected from a group of benchmark experimental tests conducted at ORNL and reported in Ref. 4. As stated in that reference, the tests were performed to provide experimental benchmark problem data suitable for assessing inelastic analysis methods and for validating computer programs. All specimens were machined from a common well-characterized heat (heat 9T2796) of type 304 stainless steel, and all tests were performed at a temperature of 593°C (1100°F).

Reference 4 presented results for four beams and four plates which were subjected to time-varying loadings, half of the tests under load-control and half under deflection-control. Only the one beam test (beam B9) and the one plate test (plate CP5), both under load-control and both devoid of so-called "precreep cycles,"* were considered in this study. Furthermore, only the portion of the loadings consisting of a short-term monotonic loading followed by a constant-load hold period was considered, for it is to only this limited type of loading that the isochronous method has straightforward application.

2.1 Test of Beam B9

Beam B9 was a simply-supported, centrally-loaded beam of uniform rectangular cross section as depicted in Fig. 1. The specimen was 50.8 mm high, 25.4 mm wide, and 0.66 m long (2 x 1 x 26 in.) and was simply supported so that the effective length was 0.61 m (24 in.). The center load was applied through a 19-mm-diam (0.75-in.) roller downward (+P) on the top surface or upward (−P) on the bottom surface as shown. The simple end supports were through 19-mm-diam (0.75-in.) rollers which passed through the beam on its centerline.

Also shown in Fig. 1 is the instrumentation used for measuring deflection, strain, and temperature. For purposes of comparison with

---

*Some of the beam and plate tests began with a short-term loading sequence which involved ten cycles of ± plastic deformation. The sequence was conducted rapidly enough to exclude significant time-dependent (creep) material behavior; thus the term "precreep cycles."

ORNL-DWG 79-7378

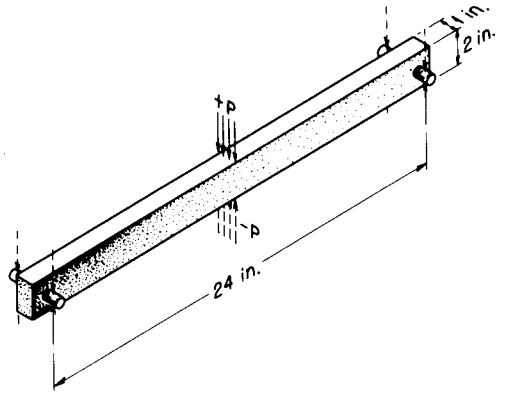

(*a*) SIMPLY-SUPPORTED BEAM SPECIMEN

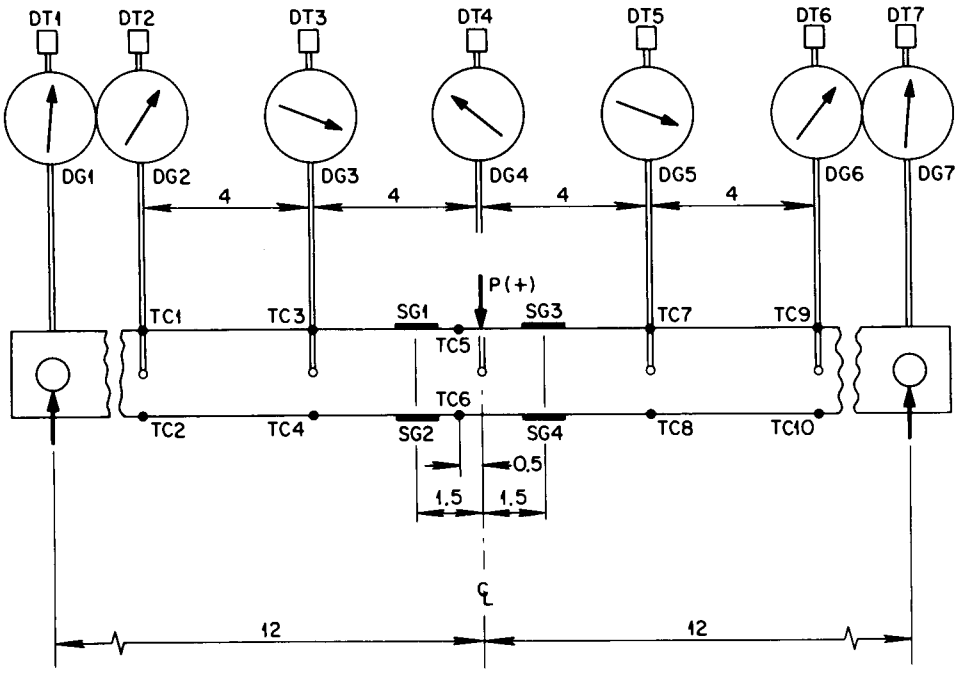

DT: DCDT
DG: DIAL GAGE
TC: THERMOCOUPLE
SG: WELDABLE RESISTANCE STRAIN GAGE

NOTE:
DIMENSIONS IN INCHES

(*b*) SCHEMATIC OF INSTRUMENTATION

Fig. 1. Test of beam B9 (in. x 25.4 = mm).

analysis, only the center DCDT* (DT4) and an average strain (computed by simple average over the four strain gages) were considered as the experimental data. Note that the weldable resistance strain gages (Ailtech Model SG425) produced no usable time-dependent strain measurements, so that the only creep data considered were center deflection measurements.

The histogram for the loading considered herein is defined as follows: (a) commence loading from zero load (this is point 1 of the histogram); (b) at constant loading rate, increase the load to 8896 N (2000 lb) in 30 sec (point 2 is the point of full load); and (c) hold load constant at 8896 N for 312 hr to reach point 3 of the loading histogram.

The measured response is summarized in Table 1. The total center deflection at histogram point 3 consisted of elastic, plastic, and creep portions of about 26, 52, and 22% respectively.

Table 1. Measured response for beam B9

Transducer[a]	Histogram point[b]	Deflection, δ (mm)	Strain, ε (%)
Center DCDT (DT4)	2	3.759	
	3	4.826	
	Creep (2–3)[c]	1.067	
Average strains (SG1 + SG2 + SG3 + SG4)/4	2		0.2603
	3		[d]

[a]Transducers are identified in Fig. 1(b).

[b]Histogram points are defined in the preceding text (subsection 2.1).

[c]Creep was assumed to begin at point 2, the conclusion of the short-time (30-sec) loading.

[d]Strain gages produced no usable time-dependent measurements.

2.2 Test of Plate CP5

Plate CP5 was a simply-supported, circular plate axisymmetrically loaded over the center portion as depicted in Fig. 2. The specimen was

*A DCDT (direct-current differential transformer) is a displacement-measuring device.

ORNL-DWG 79-7377

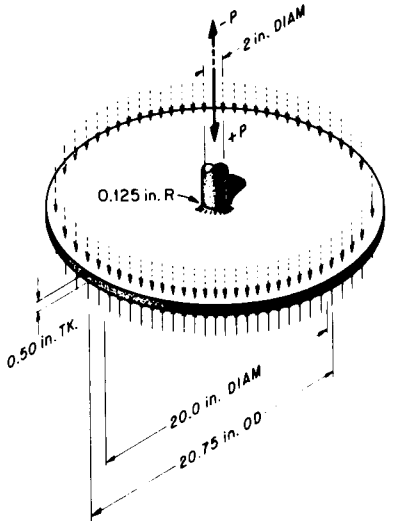

(a) SIMPLY-SUPPORTED CIRCULAR PLATE SPECIMEN

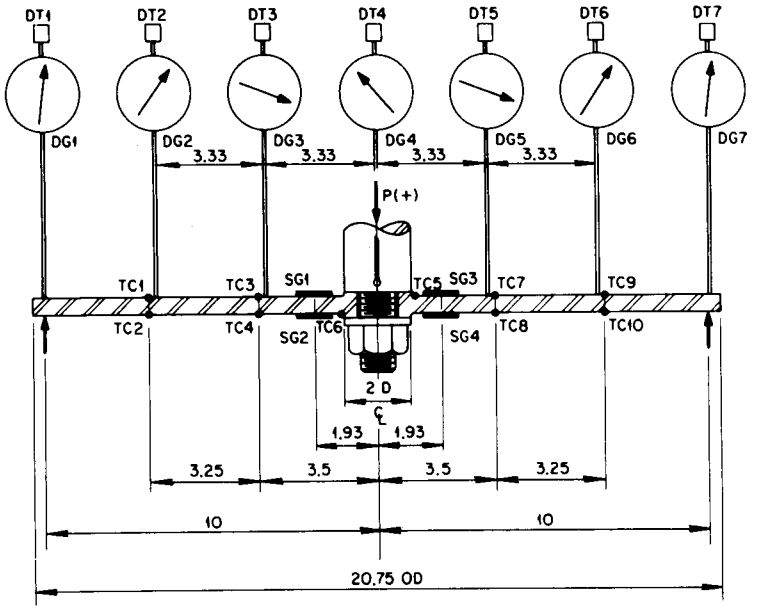

DT: DCDT
DG: DIAL GAGE
TC: THERMOCOUPLE
SG: WELDABLE RESISTANCE STRAIN GAGE

NOTE:
DIMENSIONS IN INCHES

(b) SCHEMATIC OF INSTRUMENTATION

Fig. 2. Test of plate CP5 (in. x 25.4 = mm).

12.7 mm (0.5 in.) thick and had an outside diameter of 0.527 m (20.75 in.). It was simply supported by a line of 12.7-mm-diam (0.5-in.) ball bearings on a 0.508-m-diam (20-in.) circle. Since the center load could be applied either down (+P) or up (−P), ball bearing supports were required on both the bottom and top surfaces. The center load was applied through a 50.8-mm-diam (2-in.) boss and loading bar as shown. The boss and bar arrangement provided a configuration that is adequately modeled as a 50.8-mm-diam (2-in.) solid bar, top and bottom, at the center of the plate.

Also shown in Fig. 2 is the instrumentation used in the test. Herein, as with the beam, only the center DCDT (DT4) and an average strain (computed by simple average over the four strain gages) were considered as the experimental data. Again, the Ailtech strain gages provided no usable time-dependent (creep) measurements.

The histogram for the loading was: (a) commence loading from zero load (point 1); (b) at constant loading rate, increase the load to 17,347 N (3,900 lb) in 30 sec (point 2 is the point of full load); and (c) hold load constant for 312 hr to reach point 3 of the loading histogram.

The measured response is summarized in Table 2. The total center deflection at histogram point 3 consisted of elastic, plastic, and creep portions of about 60, 15, and 25% respectively.

Table 2. Measured response for plate CP5

Transducer[a]	Histogram point[b]	Deflection, δ (mm)	Strain, ε (%)
Center DCDT (DT4)	2	2.405	
	3	3.198	
	Creep (2–3)[c]	0.793	
Average strains (SG1 + SG2 + SG3 + SG4)/4	2		0.0553
	3		[d]

[a]Transducers are identified in Fig. 2(b).

[b]Histogram points are defined in the preceding text (subsection 2.2).

[c]Creep was assumed to begin at point 2, the conclusion of the short-time (30-sec) loading.

[d]Strain gages produced no usable time-dependent measurements.

3. MATERIAL BEHAVIOR DESCRIPTIONS

This section contains a summary of the material property descriptions used in the analyses. The material data were extracted from Appendix A of Ref. 4 and consisted of elastic constants, stress-plastic-strain information, and uniaxial constant-stress creep data, all for heat 9T2796 of type 304 stainless steel and for a temperature of 593°C (1100°F). Isochronous curves were constructed based on these data.

The elastic constants used in all analyses were:

Young's modulus, $E = 149.6 \times 10^3$ MPa (21.7×10^6 psi)

and

Poisson's ratio, $\nu = 0.3$.

For consistency between detailed and isochronous solutions and for compliance with the recommendations of Ref. 1 concerning plasticity theory, a linear kinematic hardening model (thus, a bilinear elastic-plastic stress-strain curve) was used in all time-independent analyses. Though the use of a nonlinear plasticity model is theoretically acceptable for the simple problems considered herein, it was, nevertheless, concluded that the linear model was a more fitting choice considering the limited extent of this initial investigation.

3.1 Material Descriptions for Detailed Inelastic Analyses

The constitutive equations of the detailed elastic-plastic-creep analyses were those of RDT Standard F9-5T (Ref. 1) and consisted of: (1) isotropic elastic model, (2) bilinear plastic model with von Mises yield and kinematic hardening, and (3) creep model of isotropic strain-hardening. No creep-plasticity interaction rules were evoked.

The bilinear plastic properties were based on the monotonic tensile portion (first loading) from a cyclic stress strain curve conducted for a total strain range of 0.4% (peak strains = ±0.2%) and at a strain rate of 0.005/min. The maximum strain of 0.2% is reasonably

representative of the elastic-plastic strains reached in the beam test and the plate test. The plastic properties used in the detailed elastic-plastic-creep analyses (and also used in construction of the isochronous curves) were: initial yield, $\sigma_{y,o} = \sqrt{3\kappa_o} = 62.06$ MPa (9×10^3 psi) and tangent modulus, $E_m = 3/2\ EC/(E + 3/2\ C) = 4.62 \times 10^3$ MPa (0.67×10^6 psi), where κ_o and C are as defined in Ref. 1, and E is Young's modulus. Cyclic properties were not required since only monotonic loadings were considered.

The uniaxial creep strain vs time description was a tabular form which included primary and steady-state creep strains and is given in Table 3. To perform strain-hardening calculations it was necessary to develop and program an algorithm to eliminate the time variable, thus producing creep strain rate as a function of stress and creep strain. In the algorithm, linear interpolation on both the rows and columns of the matrix was adopted. The minimum (steady-state) creep rate was calculated for a given stress using the last two row entries.

3.2 Material Descriptions for Isochronous Stress-Strain Analyses

For the simplified analysis, the 312-hr isochronous stress-strain curve was generated using the bilinear elastic-plastic properties and the data matrix description for creep discussed in the previous section. Table 4 designates the elastic, plastic, and creep strain components of the isochronous curve. The elastic strain was calculated as σ/E; the plastic strain, as $(\sigma - \sigma_{y,o})/E_p$, where $E_p = 3/2\ C$ and $\sigma > \sigma_{y,o}$; and the creep strain, by linear interpolation (with time) between the 200-hr and 500-hr columns of the creep matrix. Figure 3 is a composite of the components of the isochronous curve. The resultant curve, Fig. 3(d), appears as a bilinear-slightly-nonlinear σ-ε curve. At 83 MPa (12×10^3 psi) the proportions of the elastic, plastic, and creep components are about 9, 70, and 21% respectively.

The constitutive equations of the isochronous stress-strain analyses were the same as used in the elastic-plastic portion of the detailed analyses; that is, an isotropic elastic model and a bilinear, kinematic-hardening plastic model were employed. Bilinearizing the isochronous

Table 3. Uniaxial creep strain (%) matrix for type 304 stainless steel (heat 9T2796) at 593°C (1100°F)

Stress[a] (1000 psi)	Time (hr)												
	1	2	5	10	20	50	100	200	500	1000	2000	5000	10,000
1	0.00006	0.00010	0.00022	0.00040	0.00060	0.00067	0.00078	0.00098	0.00150	0.00200	0.00250	0.00320	0.00370
2	0.00018	0.00032	0.00065	0.00100	0.00140	0.00170	0.00210	0.00270	0.00400	0.00470	0.00550	0.00700	0.00800
3	0.00036	0.00070	0.00120	0.00182	0.00250	0.00300	0.00355	0.00450	0.00700	0.00830	0.01000	0.01200	0.01400
4	0.00060	0.00115	0.00187	0.00280	0.00400	0.00475	0.00575	0.00750	0.01000	0.01250	0.01500	0.01900	0.02150
5	0.00095	0.00173	0.00275	0.00410	0.00570	0.00700	0.00830	0.01010	0.01500	0.01870	0.02250	0.02750	0.03150
6	0.00140	0.00250	0.00400	0.00575	0.00775	0.00980	0.01200	0.01600	0.02220	0.02750	0.03200	0.03950	0.04500
7	0.00210	0.00355	0.00550	0.00800	0.01070	0.01375	0.01700	0.02250	0.03100	0.03800	0.04700	0.05800	0.06700
8	0.00290	0.00485	0.00765	0.01070	0.01450	0.01950	0.02400	0.03100	0.04300	0.05300	0.06800	0.08900	0.10500
9	0.00400	0.00650	0.01000	0.01400	0.01900	0.02650	0.03300	0.04350	0.06000	0.07500	0.10100	0.14000	0.16500
10	0.00515	0.00830	0.01300	0.01815	0.02400	0.03600	0.04700	0.06000	0.08300	0.10700	0.14000	0.21500	0.29000
11	0.00650	0.01035	0.01650	0.02300	0.03150	0.04900	0.06500	0.08500	0.12000	0.15300	0.19500	0.31250	0.50000
12	0.00750	0.01240	0.02000	0.02900	0.04200	0.06500	0.08900	0.11500	0.16500	0.21000	0.27000	0.43750	0.68000
13	0.00910	0.01475	0.02450	0.03600	0.05400	0.08500	0.11700	0.15500	0.22000	0.28500	0.37200	0.57500	0.90000
14	0.01150	0.01720	0.02800	0.04200	0.06750	0.10750	0.15200	0.20250	0.29500	0.38000	0.49400	0.75500	1.16500
15	0.01355	0.01965	0.03350	0.05300	0.08500	0.13350	0.19100	0.25950	0.38000	0.49300	0.62500	0.98500	1.48000
16	0.01515	0.02220	0.03800	0.06100	0.10300	0.16500	0.24200	0.32250	0.48000	0.62500	0.80000	1.25000	1.90000
17	0.01700	0.02450	0.04500	0.07200	0.11600	0.20250	0.29800	0.39400	0.60000	0.80000	1.04500	1.60000	2.50000
18	0.02500	0.03500	0.05600	0.08600	0.14000	0.24000	0.35500	0.51000	0.77500	1.05000	1.40000	2.20000	3.50000
19	0.02800	0.04200	0.08000	0.12500	0.19000	0.30000	0.45000	0.65000	0.99000	1.40000	2.00000	2.97500	
20	0.03200	0.05000	0.09500	0.16000	0.24000	0.38500	0.57500	0.82000	1.27500	1.95000	3.00000		
21	0.03600	0.06000	0.12200	0.20000	0.31000	0.49000	0.71000	1.02500	1.67500	2.70000			
22	0.04000	0.07700	0.15500	0.25000	0.39000	0.62000	0.88500	1.31000	2.25000				
23	0.05000	0.09500	0.19500	0.31000	0.48000	0.77500	1.11100	1.68500	3.00000				
24	0.06500	0.12000	0.23500	0.38000	0.60000	0.95500	1.40000	2.17500					
25	0.08000	0.15000	0.29000	0.47000	0.72500	1.20000	1.77500	2.80000					
26	0.09000	0.17700	0.35000	0.57500	0.90000	1.51000	2.25000	3.50000					
27	0.11500	0.22000	0.42300	0.70000	1.10000	1.90000	2.80000						
28	0.14500	0.26000	0.50000	0.85000	1.35500	2.34000	3.42000						
29	0.18000	0.32500	0.61500	1.03500	1.68000	2.87500							
30	0.22500	0.40000	0.77000	1.25500	2.07500	3.42500							
31	0.28000	0.50500	0.98000	1.54500	2.55000								
32	0.35000	0.63200	1.25000	1.90000	3.06500								
33	0.43500	0.80000	1.57500	2.31000									
34	0.53500	0.98000	1.92500	2.80000									
35	0.65500	1.21500	2.31000	3.32500									

[a]1000 psi × 6.895 = MPa.

Table 4. Strain components (%) of the 312-hr isochronous stress-strain curve for type 304 stainless steel (heat 9T2796) at 593°C (1100°F)

Stress (1000 psi)[a]	Elastic Strain	Plastic Strain	Creep Strain	Total Strain
5	0.0230	0	0.0119	0.0349
6	0.0276	0	0.0183	0.0459
7	0.0322	0	0.0257	0.0579
8	0.0369	0	0.0355	0.0724
9	0.0415	0	0.0497	0.0912
10	0.0461	0.1444	0.0686	0.2591
11	0.0507	0.2890	0.0981	0.4378
12	0.0553	0.4337	0.1337	0.6227
13	0.0599	0.5783	0.1793	0.8175
14	0.0645	0.7230	0.2370	1.0245
15	0.0691	0.8676	0.3045	1.2412

[a]1000 psi x 6.895 = MPa.

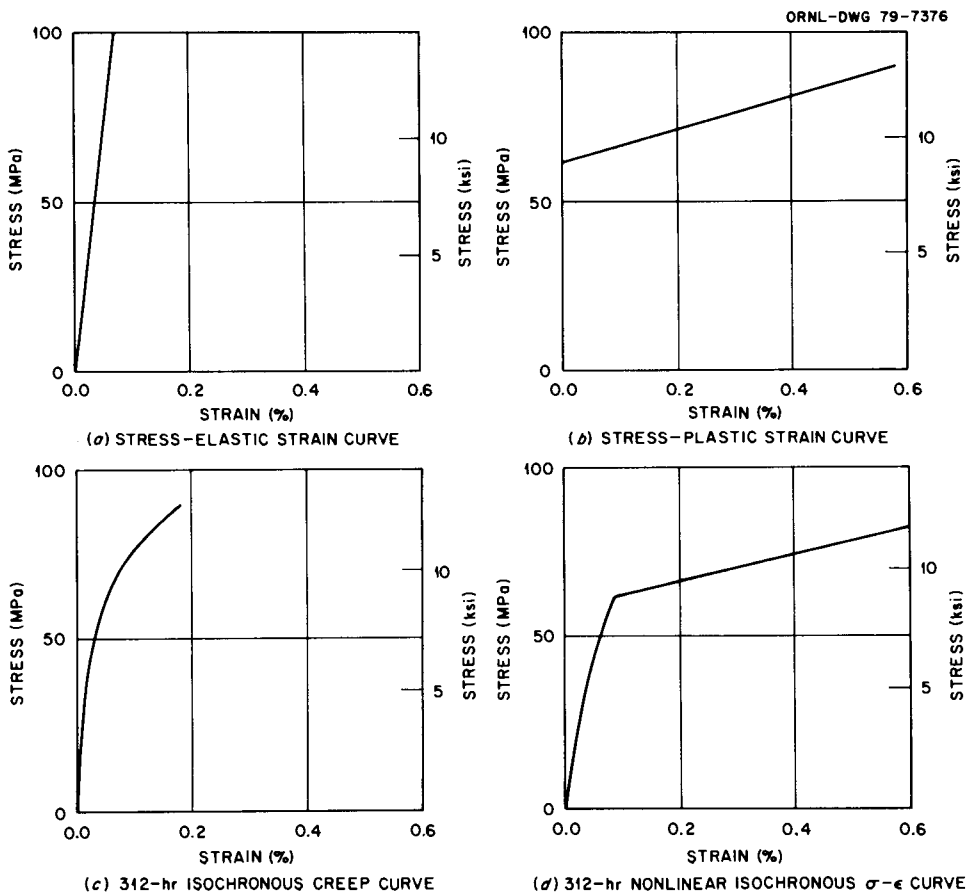

Fig. 3. Components of the 312-hr isochronous stress-strain curve for type 304 stainless steel (heat 9T2796) at 593°C (1100°F).

stress-strain curve of Fig. 3(d) involved only a "mild" idealization; also, little sensitivity of $\sigma_{y,o}$ and E_m to the choice of ε_{max} was exhibited. A value of ε_{max} equal to 0.5% was selected and bilinearizing of the curve yielded:

$$\sigma_{y,o} = 60.96 \text{ MPa } (8841 \text{ psi})$$

and

$$E_m = 3.719 \times 10^3 \text{ MPa } (0.5394 \times 10^6 \text{ psi}).$$

Thus, the effects of including creep strains in the plastic properties were to reduce the yield stress by about 2% and to reduce the tangent modulus (and plastic modulus) by about 20%. Figure 4 shows the original bilinear elastic-plastic curve, the "nonlinear" 312-hr isochronous stress-strain curve, and the bilinear 312-hr isochronous stress-strain curve.

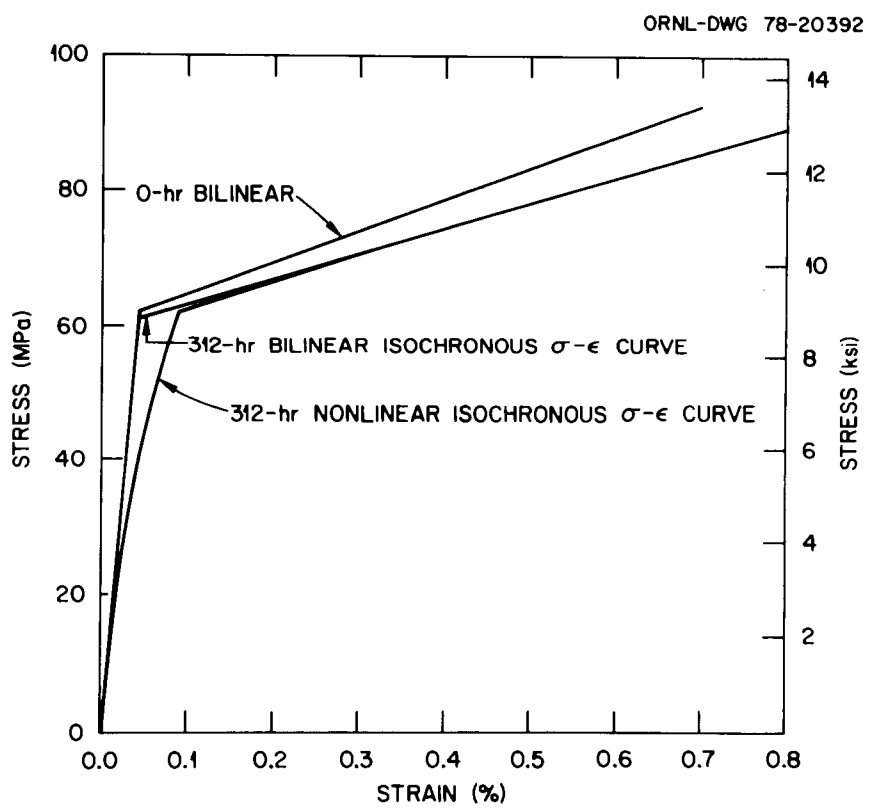

Fig. 4. Details of the 0-hr and 312-hr isochronous σ-ε curves.

4. DETAILED SOLUTIONS

The detailed elastic-plastic-creep solutions for the beam and plate problem were obtained using the finite-element computer program CREEP-PLAST II.[5] The specimens and their idealizations are detailed in Figs. 5 and 6. The plane-stress elements of the beam were constant-strain triangles. The axisymmetric elements of the plate were three-node revolved triangles. Half-symmetry was employed for the beam model.

Solutions were calculated in an incremental fashion with elastic-plastic strains being incorporated through a tangent-stiffness algorithm and creep strains through an initial-strain algorithm. Each analysis increment contained one or more solutions to the assembled matrix equations of the system of finite elements. Each solution repetition was roughly equivalent (in terms of total computations) to an elastic solution of the problem. A summary of the solution requirements for the beam and plate problems is given in Table 5.

4.1 Detailed Solution of Beam B9

Following the same convention as in Table 1 of Sect. 2.1, the computed solution for beam B9 is given in Table 6. The total center deflection at histogram point 3 consisted of elastic, plastic, and creep portions of about 22, 44, and 34% respectively.

To provide whole-field displays of the analysis results, stress and strain contours were constructed using the CREEP-PLAST Graphics Package.[6] The σ_{xx} (longitudinal) component of stress calculated for histogram point 3 is displayed in Fig. 7; the ε_{xx} component of strain, in Fig. 8. A 10.2-cm (4-in.) portion of the beam is considered in the figures.

The dependence of stress and strain on both x and y and the magnitudes and the gradients of the quantities can be better understood and visualized with the aid of such plots. The slight antisymmetry (with respect to the neutral surface) of the contours may be attributed to the antisymmetry of the grid and to the point of load application on the surface (Fig. 5). The distortions near the transverse line of symmetry are the most severe and may be traced to the smoothing algorithm in

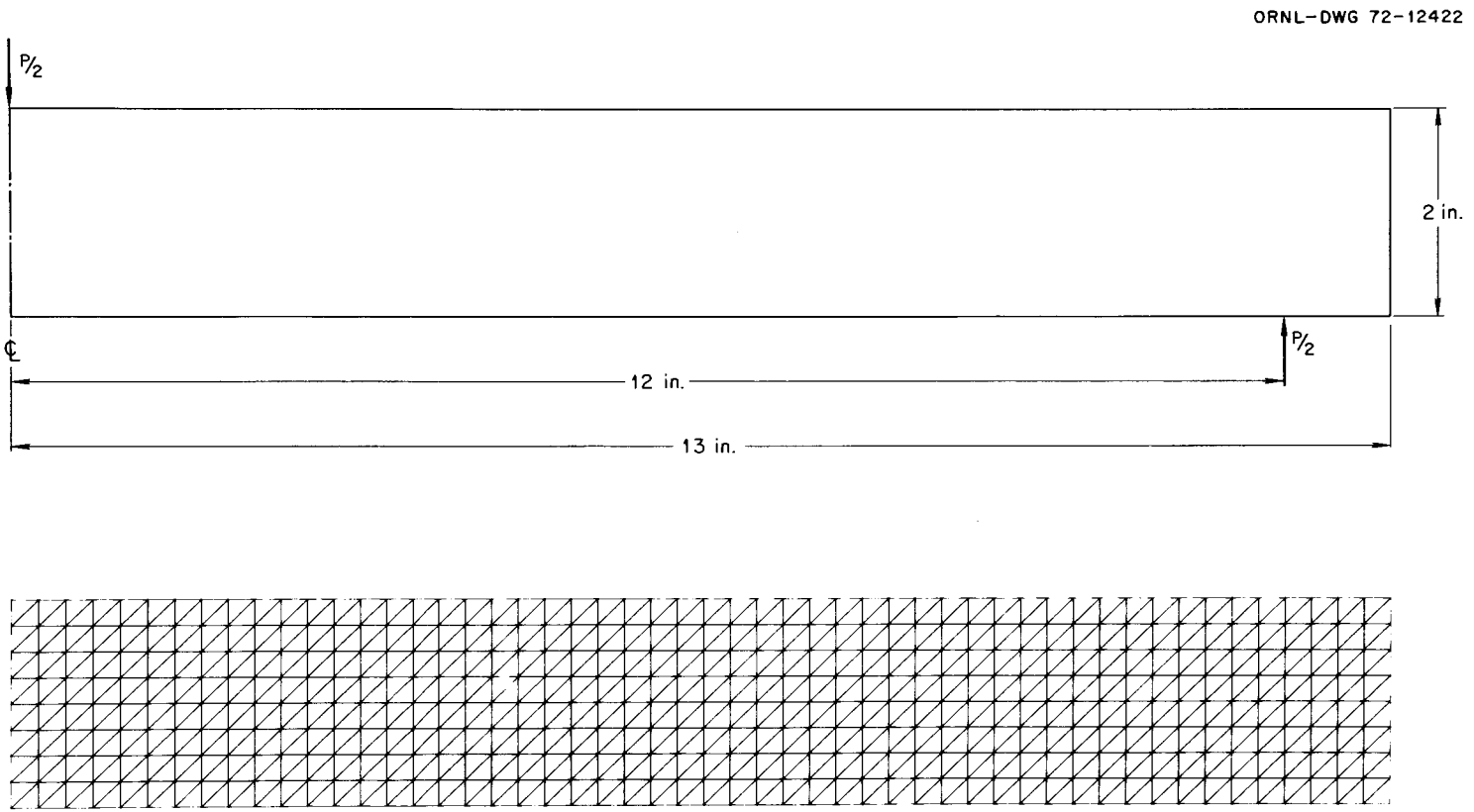

FINITE ELEMENT IDEALIZATION
832 ELEMENTS
477 NODES

Fig. 5. Finite element idealization of beam B9 (in. x 25.4 = mm).

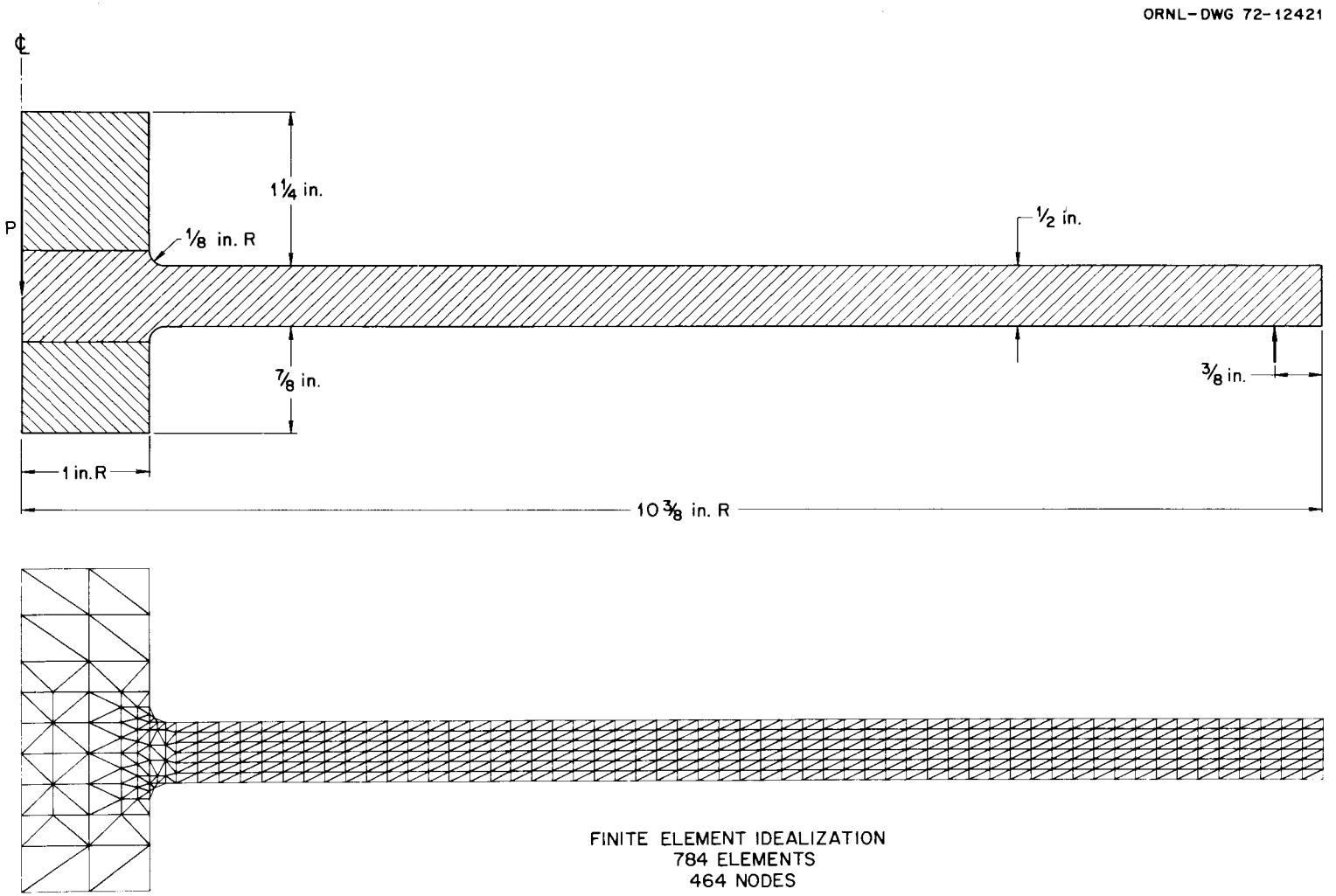

Fig. 6. Finite element idealization of plate CP5 (in. x 25.4 = mm).

Table 5. Summary of requirements for the beam and plate solutions by CREEP-PLAST II using a detailed elastic-plastic-creep model

Solution type	Specimen	Solution repetitions[a]	CPU[b] time (sec)
Elastic-plastic[c]	Beam B9	37	237
	Plate CP5	37	351
Creep[d]	Beam B9	66	423
	Plate CP5	66	627

[a]In CREEP-PLAST II solutions, a repetition is a full assemblage and solution of the global stiffness equations. Solution repetitions to include creep require essentially the same computational effort as repetitions to include short-term elastic-plastic behavior.

[b]CPU time is computation time on the ORNL IBM 360/91 computer.

[c]Solutions were for the short-time load application (point 1 to point 2 in the histograms).

[d]Solutions were for the constant-load hold period of 312 hr (point 2 to point 3).

Table 6. Summary of the solution (computed at the transducer locations) for beam B9 using a detailed elastic-plastic-creep model

Transducer[a]	Histogram point[b]	Deflection, δ (mm)	Strain, ε (%)
Center DCDT (DT4)	2	3.038	
	3	4.572	
	Creep (2–3)[c]	1.534	
Average strains (SG1 + SG2 + SG3 + SG4)/4	2		0.2869
	3		0.4276
	Creep (2–3)		0.1407

[a]Transducers are identified in Fig. 1(b).

[b]Histogram points are defined in subsection 2.1.

[c]Creep was assumed to begin at point 2, the conclusion of the short-time (30-sec) loading.

ORNL-DWG 78-20391

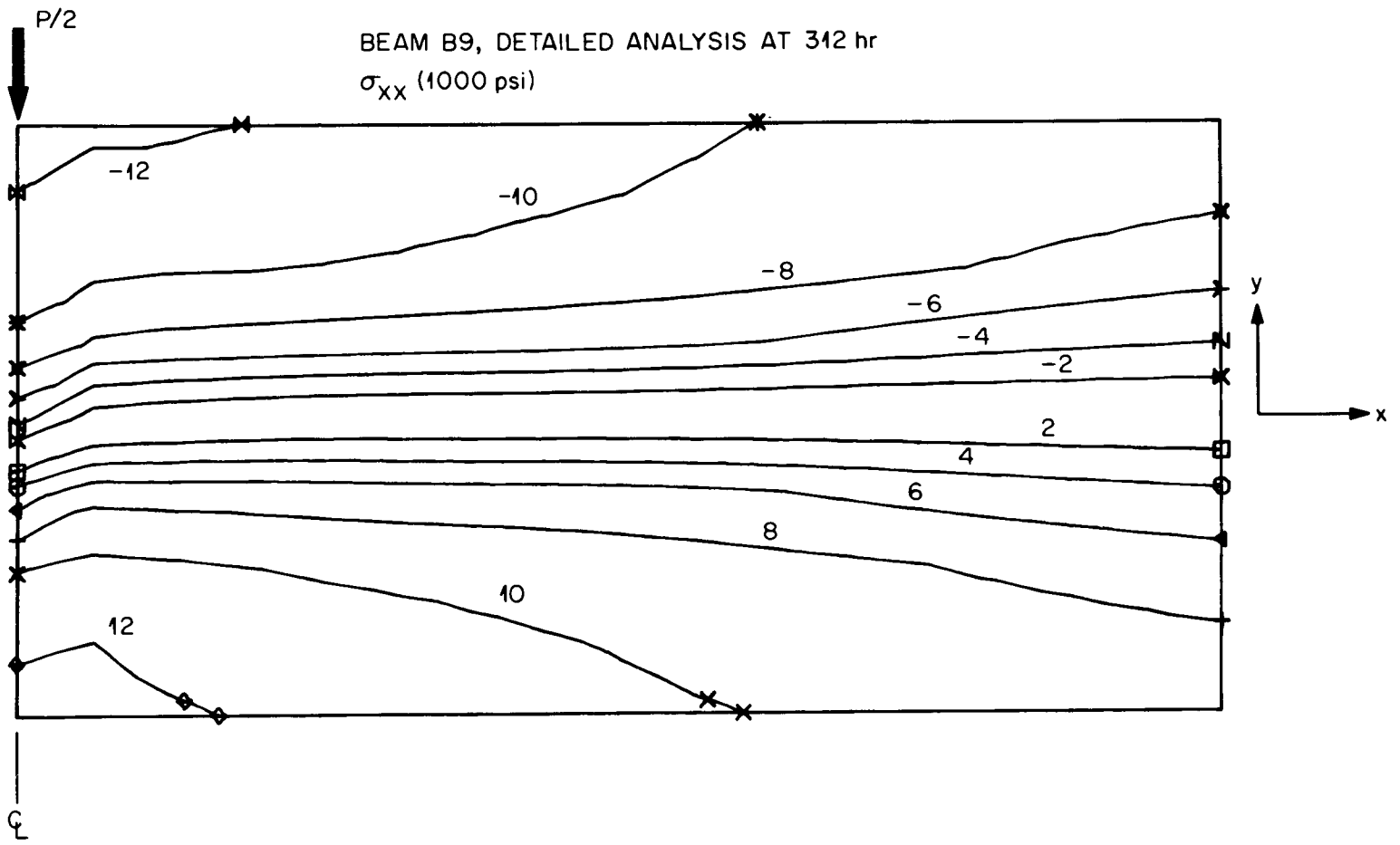

Fig. 7. The σ_{xx} stress contours at load point 3 for beam B9. Solution was calculated using a detailed elastic-plastic-creep model in CREEP-PLAST II. Stress is designated in 1000 psi (1000 psi x 6.895 = MPa).

ORNL-DWG 78-20390

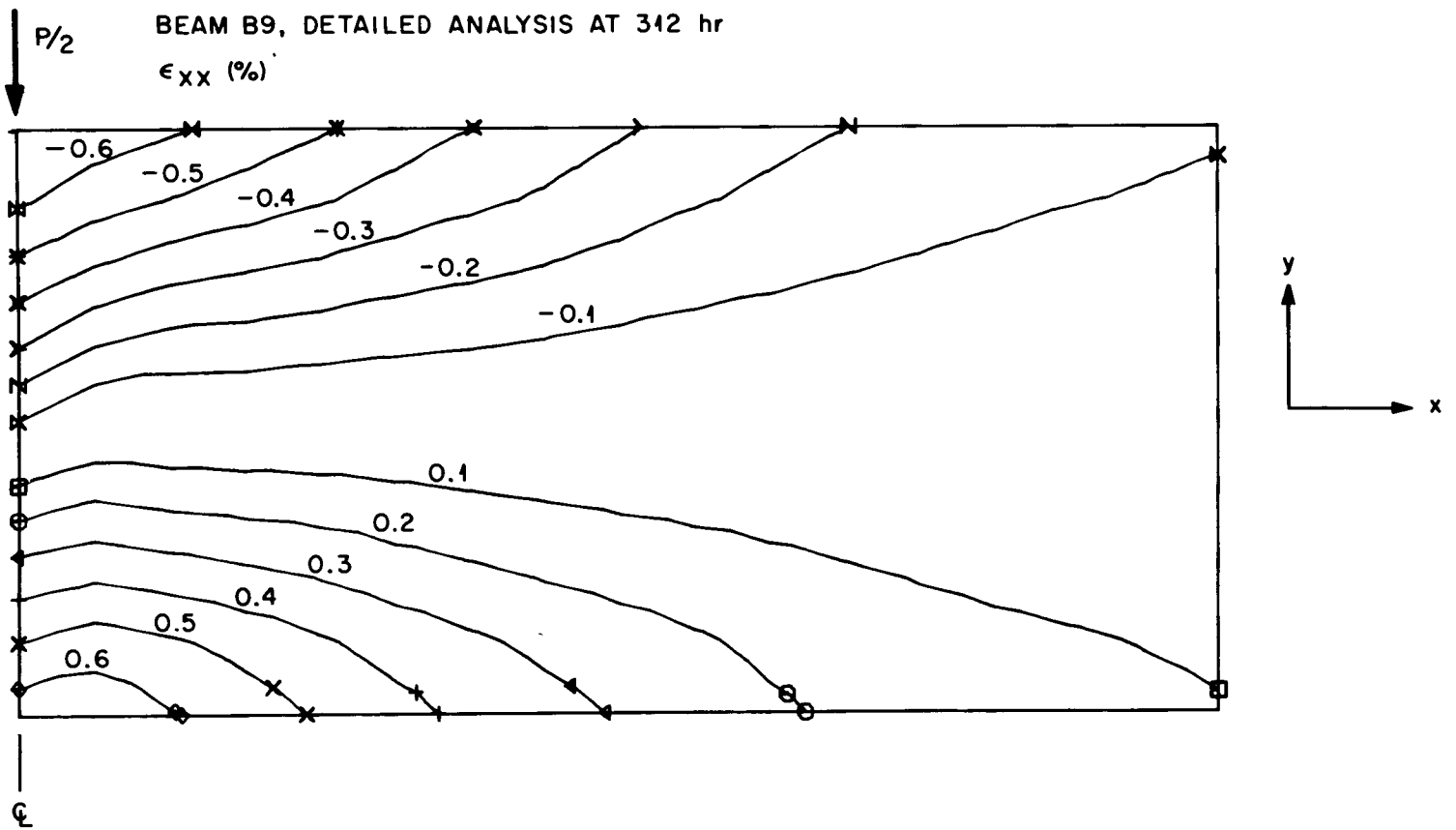

Fig. 8. The ε_{xx} total strain contours at load point 3 for beam B9. Solution was calculated using a detailed elastic-plastic-creep model in CREEP-PLAST II. Strain is designated in %.

program CØNTØUR-PLØT (see Ref. 6). The smoothing breaks down, somewhat, on such boundaries.

4.2. Detailed Solution of Plate CP5

The computed solution for plate CP5 is given in Table 7. The total center deflection at histogram point 3 consisted of elastic, plastic, and creep portions of about 48, 18, and 34% respectively.

Table 7. Summary of the solution (computed at the transducer locations) for plate CP5 using a detailed elastic-plastic-creep model

Transducer[a]	Histogram point[b]	Deflection, δ (mm)	Strain, ε (%)
Center DCDT (DT4)	2	2.230	
	3	3.399	
	Creep (2–3)[c]	1.169	
Average strains (SG1 + SG2 + SG3 + SG4)/4	2		0.0729
	3		0.1171
	Creep (2–3)		0.0442

[a]Transducers are identified in Fig. 2(b).

[b]Histogram points are defined in subsection 2.2.

[c]Creep was assumed to begin at point 2, the conclusion of the short-time (30-sec) loading.

Stress and strain contours (at point 3) are given in Figs. 9–12 for σ_{rr}, $\sigma_{\theta\theta}$, ε_{rr}, and ε_{zz} respectively. A portion of the plate (see Fig. 6) with inside radius of 12.7 mm (0.5 in.) and outside radius of 56.1 mm (2.208 in.) and excluding the loading assembly is considered in the figures.

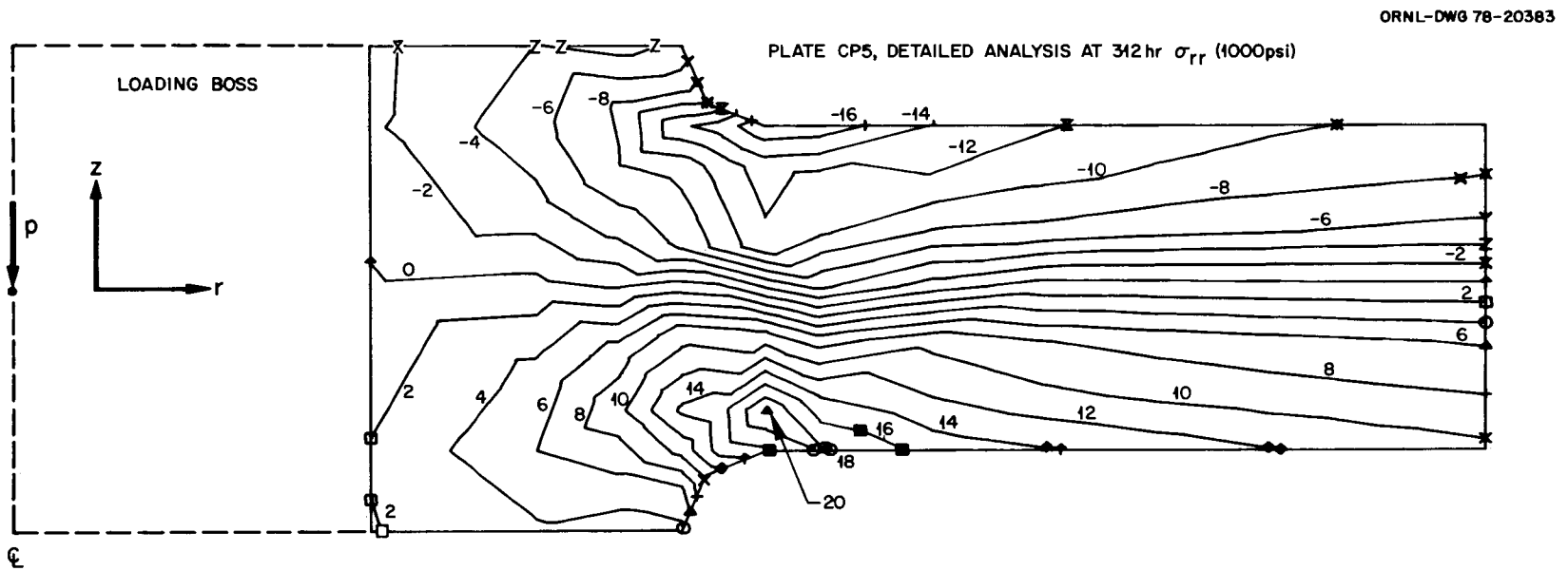

Fig. 9. The σ_{rr} stress contours at load point 3 for plate CP5. Solution was calculated using a detailed elastic-plastic-creep model in CREEP-PLAST II. Stress is designated in 1000 psi (1000 psi x 6.895 = MPa).

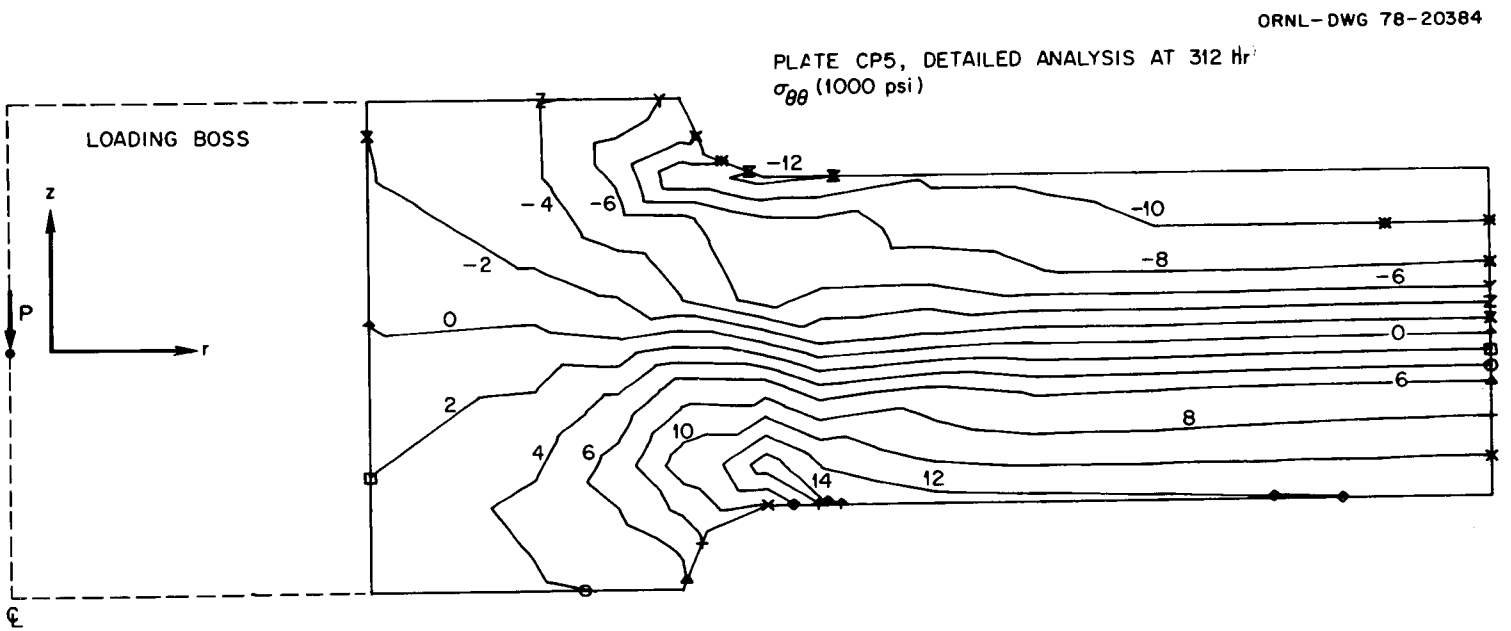

Fig. 10. The $\sigma_{\theta\theta}$ stress contours at load point 3 for plate CP5. Solution was calculated using a detailed elastic-plastic-creep model in CREEP-PLAST II. Stress is designated in 1000 psi (1000 psi x 6.895 = MPa).

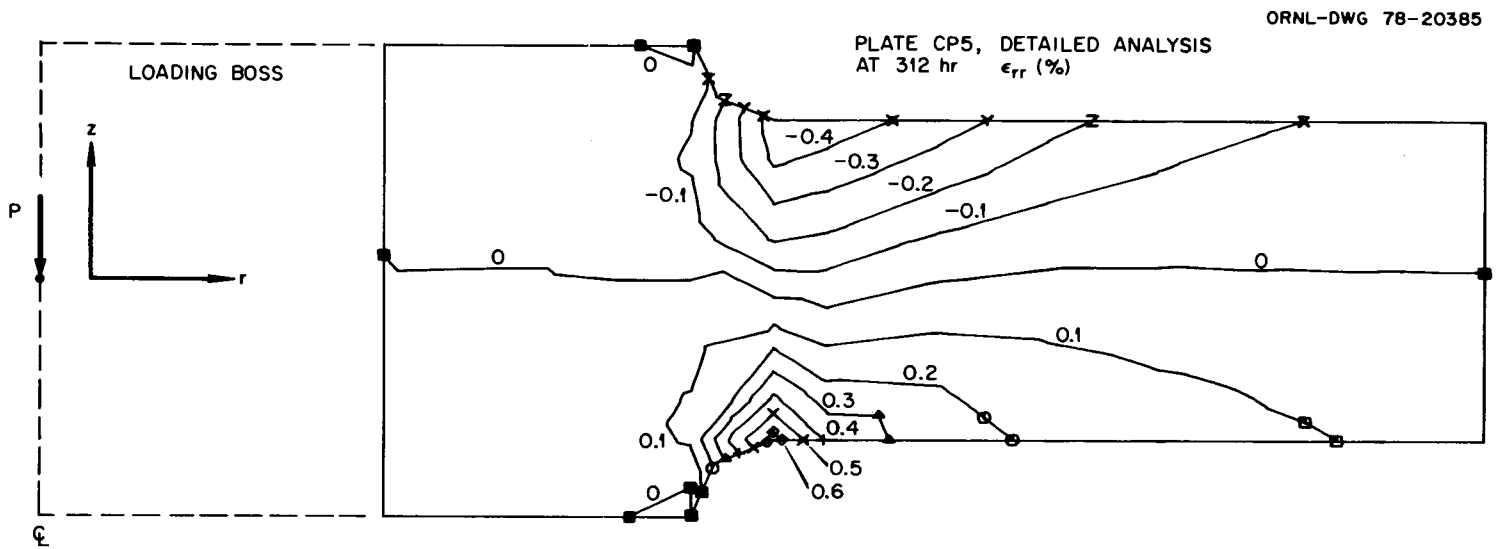

Fig. 11. The ε_{rr} total strain contours at load point 3 for plate CP5. Solution was calculated using a detailed elastic-plastic-creep model in CREEP-PLAST II. Strain is designated in %.

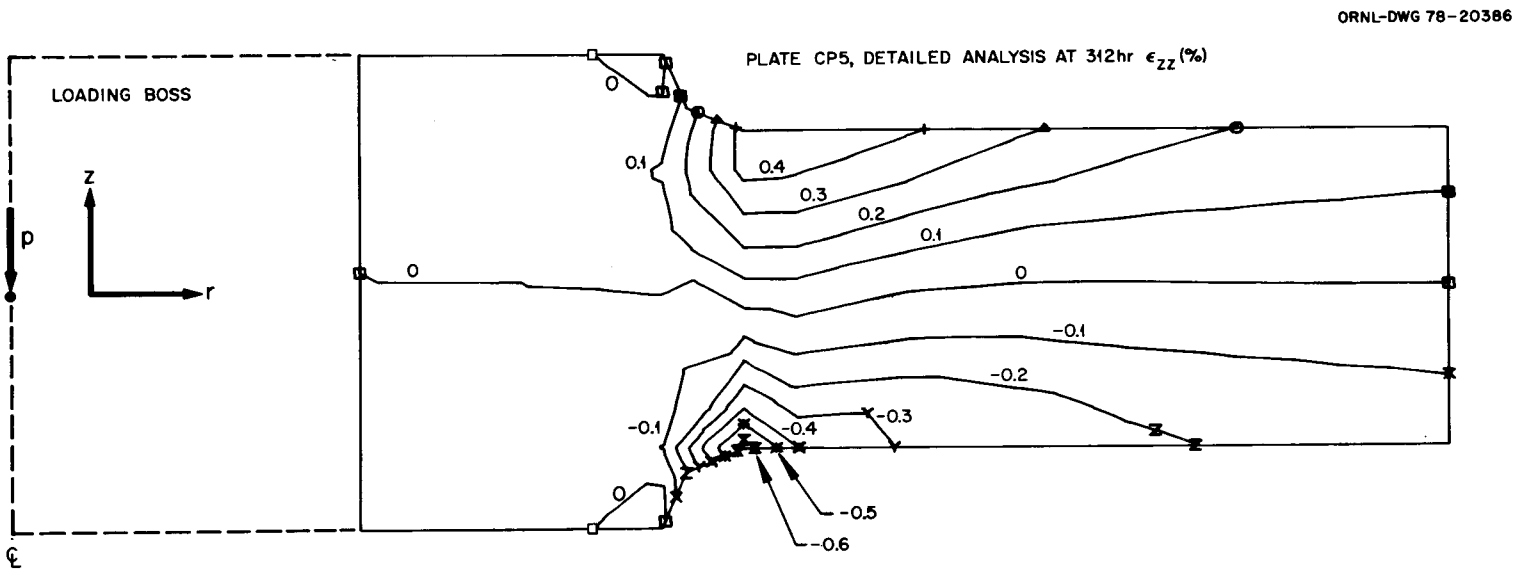

Fig. 12. The ε_{zz} total strain contours at load point 3 for plate CP5. Solution was calculated using a detailed elastic-plastic-creep model in CREEP-PLAST II. Strain is designated in %.

5. ISOCHRONOUS SOLUTIONS

The isochronous stress-strain solutions were likewise obtained using CREEP-PLAST II. The spatial idealizations for the beam and plate (see Figs. 5 and 6) were the same used in the detailed analyses. The material properties were those based on the bilinear, 312-hr isochronous curve discussed in Sect. 3.2. As with the detailed analyses (see Table 5) a total of 37 solution repetitions were employed for load application, and the computation times were very close to those reported in Table 5 for the elastic-plastic portion only of the detailed solutions.

5.1 Isochronous Stress-Strain Solution of Beam B9

The isochronous solution for beam B9 is given in Table 8. These results are comparable to the experimental data of Table 1 and the detailed solution of Table 6. The σ_{xx} and ε_{xx} contours (at point 3) are displayed in Figs. 13 and 14 respectively.

For the isochronous solution, the total center deflection at histograms point 3 consisted of elastic, plastic, and creep portions of about 26, 54, and 20% respectively.

5.2 Isochronous Stress-Strain Solution of Plate CP5

The isochronous solution is given in Table 9. These results are comparable to the experimental data in Table 2 and the detailed solution of Table 7. The σ_{rr}, $\sigma_{\theta\theta}$, ε_{rr}, and ε_{zz} contours at point 3 are displayed in Figs. 15 to 18 respectively. As with previous Figs. 9 to 12, only a portion of the plate is considered.

For the isochronous solution, the total center deflection at histogram point 3 consisted of elastic, plastic, and creep portions of about 71, 26, and 3% respectively. The small percentage for the creep portion reflects the fact that the elastic-plastic solution obtained using the 312-hr isochronous stress-strain curve was not very different from the elastic-plastic solution obtained using the 0-hr stress-strain curve. The softening of the plastic properties in the 312-hr representation caused only 13 additional finite elements to yield; that is, 203 of 784 elements

Table 8. Summary of the solution (computed at the transducer locations) for beam B9 using an isochronous stress-strain model

Transducer[a]	Histogram point[b]	Deflection, δ (mm)	Strain, ε (%)
Center DCDT (DT4)	2	3.038[c]	
	3	3.800	
	Creep (2–3)[d]	0.762[e]	
Average strains (SG1 + SG2 + SG3 + SG4)/4	2		0.2869[c]
	3		0.3796
	Creep (2–3)		0.0927[e]

[a]Transducers are identified in Fig. 1(b).

[b]Histogram points are defined in subsection 2.1.

[c]These are the 0-hr isochronous answers and are identical to the elastic-plastic answer reported in Table 6.

[d]Creep was assumed to begin at point 2, the conclusion of the short-time (30-sec) loading.

[e]The creep was computed as the difference between the 312-hr and 0-hr isochronous answers.

Table 9. Summary of the solution (computed at the transducer locations) for plate CP5 using an isochronous stress-strain model

Transducer[a]	Histogram point[b]	Deflection, δ (mm)	Strain, ε (%)
Center DCDT (DT4)	2	2.230[c]	
	3	2.306	
	Creep (2–3)[d]	0.076[e]	
Average strains (SG1 + SG2 + SG3 + SG4)/4	2		0.0729[c]
	3		0.0740
	Creep (2–3)		0.0011[e]

[a]Transducers are identified in Fig. 2(b).

[b]Histogram points are defined in subsection 2.2.

[c]These are the 0-hr isochronous answers and are identical to the elastic-plastic answer reported in Table 7.

[d]Creep was assumed to begin at point 2, the conclusion of the short-time (30-sec) loading.

[e]The creep was computed as the difference between the 312-hr and 0-hr isochronous answers.

ORNL–DWG 78–20389A

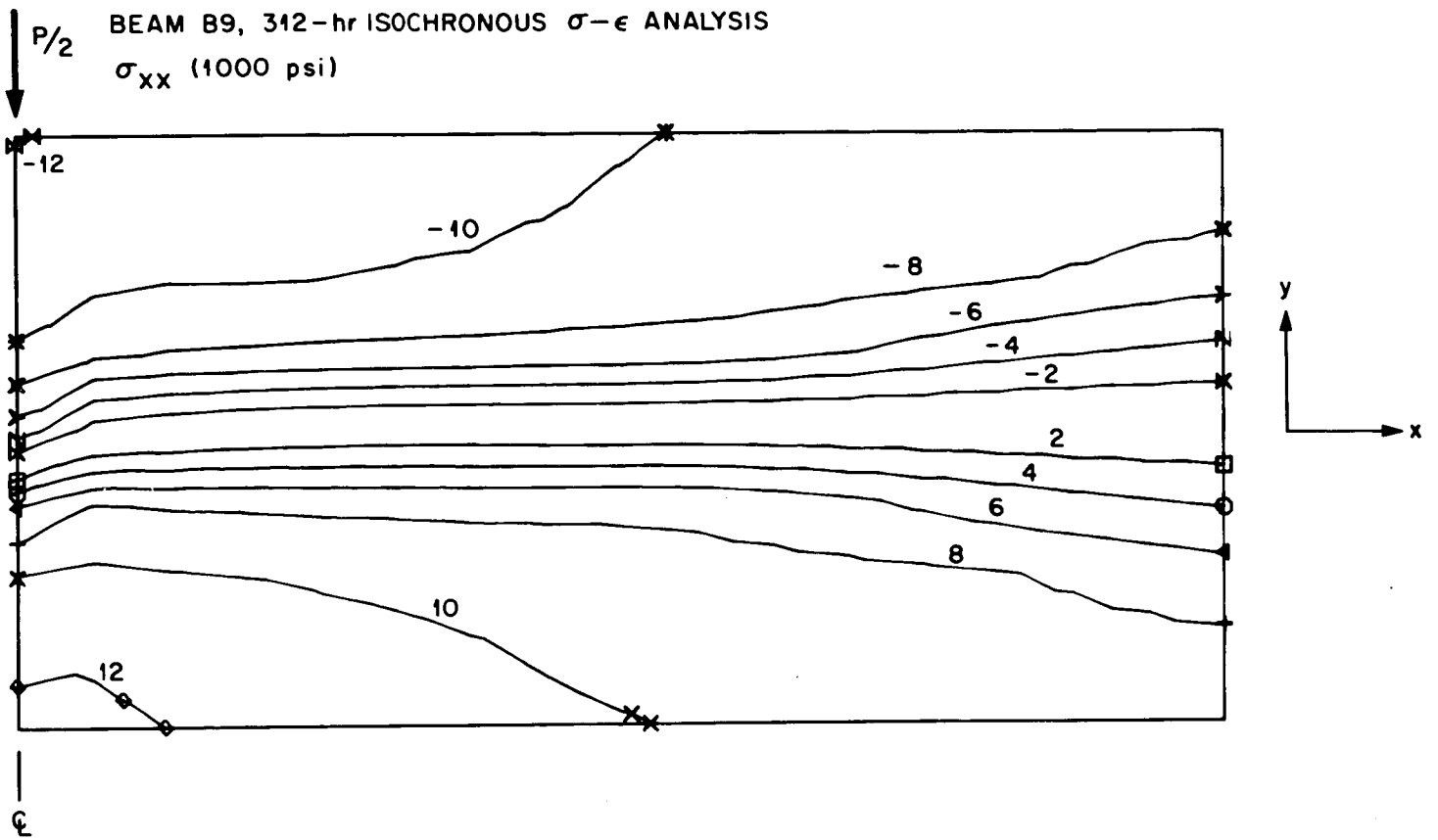

Fig. 13. The σ_{xx} stress contours at load point 3 for beam B9. Solution was calculated using an approximate isochronous σ–ε model in CREEP-PLAST II. Stress is designated in 1000 psi (1000 psi x 6.895 = MPa).

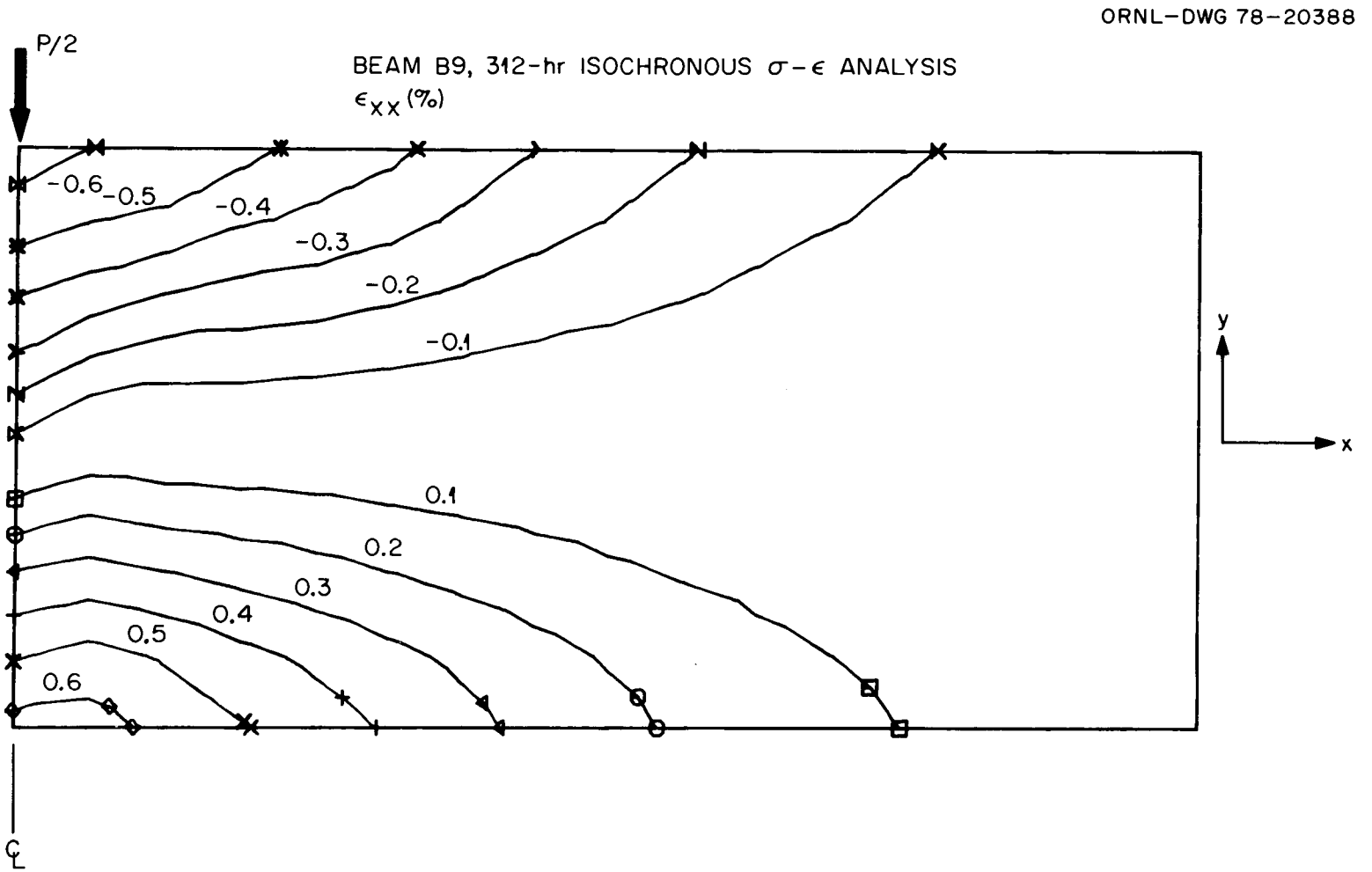

Fig. 14. The ε_{xx} total strain contours at load point 3 for beam B9. Solution was calculated using an approximate isochronous σ-ε model in CREEP-PLAST II. Strain is designated in %.

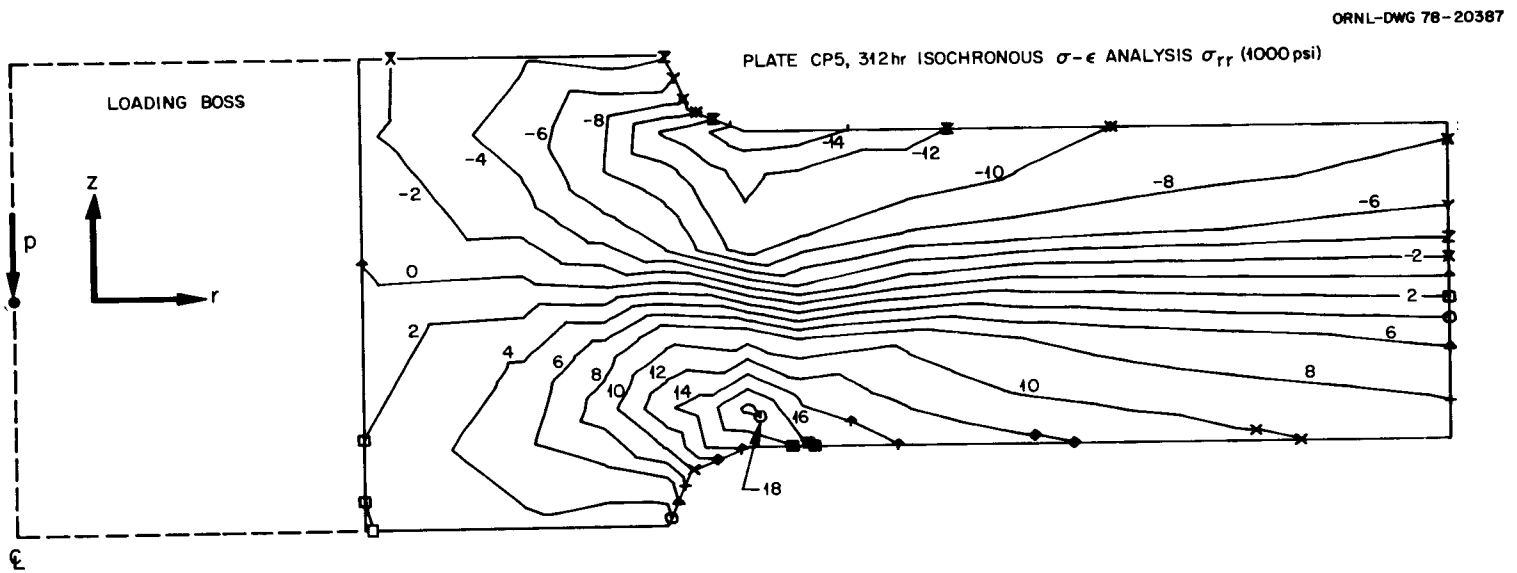

Fig. 15. The σ_{rr} stress contours at load point 3 for plate CP5. Solution was calculated using an approximate isochronous σ-ε model in CREEP-PLAST II. Stress is designated in 1000 psi (1000 psi x 6.895 = MPa).

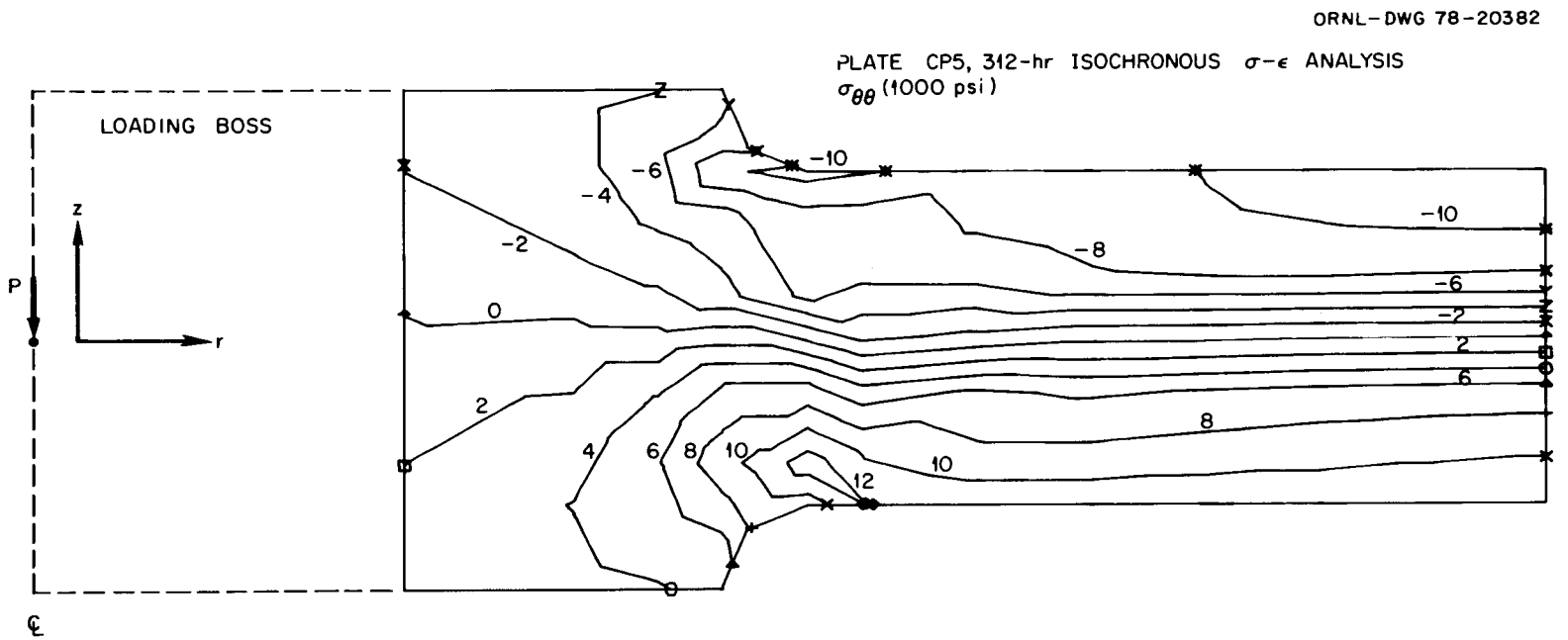

Fig. 16. The $\sigma_{\theta\theta}$ stress contours at load point 3 for plate CP5. Solution was calculated using an approximate isochronous σ-ε model in CREEP-PLAST II. Stress is designated in 1000 psi (1000 psi x 6.895 = MPa).

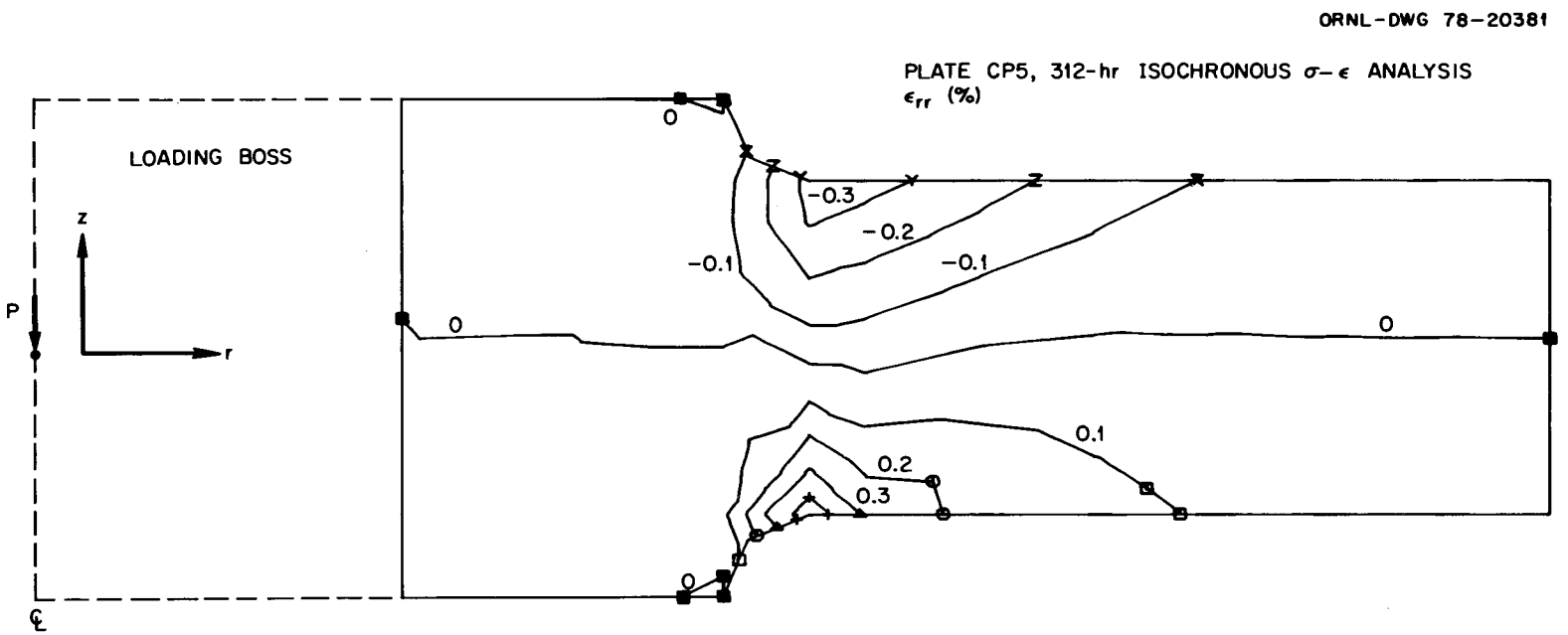

Fig. 17. The ε_{rr} total strain contours at load point 3 for plate CP5. Solution was calculated using an approximate isochronous σ-ε model in CREEP-PLAST II. Strain is designated in %.

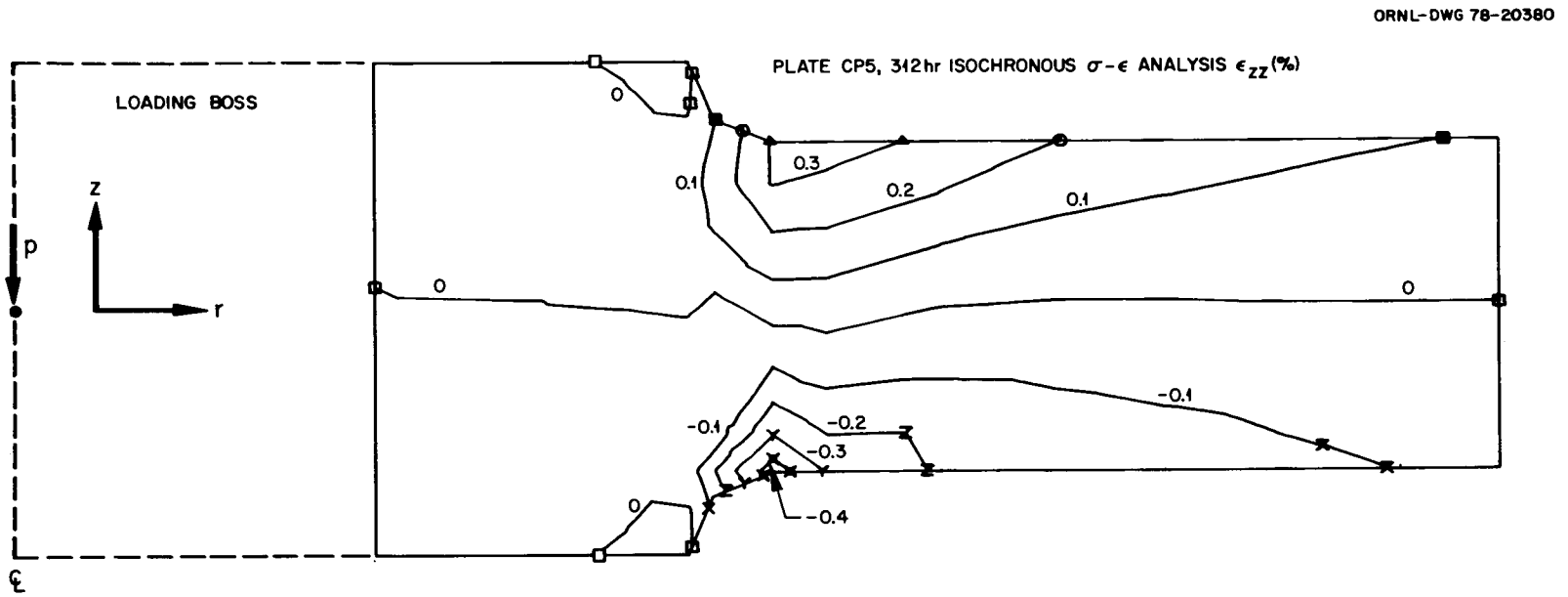

Fig. 18. The ε_{zz} total strain contours at load point 3 for plate Solution was calculated using an approximate isochronous σ-ε model in CREEP-PLAST II. Strain is designated in %.

yielded when the 0-hr curve was used, while 216 of 784 yielded when the 312-hr curve was used.

6. COMPARISON OF SOLUTIONS

It is of interest to compare the solutions calculated by the isochronous stress-strain method to experimental data and to the detailed elastic-plastic-creep solutions. Comparisons to actual test data help answer questions concerning the adequacy of the method: What measure of validity can be assigned to the method? Comparison of the isochronous solutions to detailed elastic-plastic-creep solutions is logical since the isochronous stress-strain model is brought about through simplifications of the more detailed model; one would expect the potential for accuracy of the simplified method to be bounded by that of the detailed method. Additional comparisons between experimental data and the detailed solutions are included herein for reference and completeness.

A "quick-look" comparison among the two solutions and the data is provided through Figs. 19 and 20. Figure 19 compares answers in terms of center deflection vs load for beam B9; Fig. 20, for plate CP5.

6.1 Comparison of Solutions to Test Data

6.1.1 Beam B9

The detailed elastic-plastic-creep solution and the isochronous stress-strain solution are compared to test data in Table 10. This information was determined based on results presented in Tables 1, 6, and 8. Since the strain gages provided no usable time-dependent measurements, it is impossible to quantify errors in the creep strain solutions.

6.1.2 Plate CP5

The two solutions are compared to test data in Table 11. This information was determined based on results presented in Tables 2, 7, and 9. Again, errors in the creep strain solutions cannot be quantified.

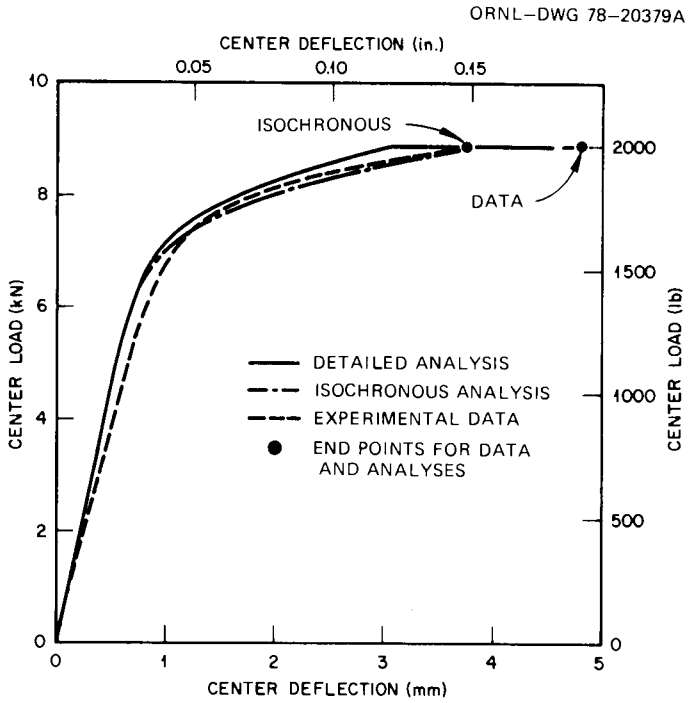

Fig. 19. Comparison among solutions and data in terms of center deflection vs load for beam B9.

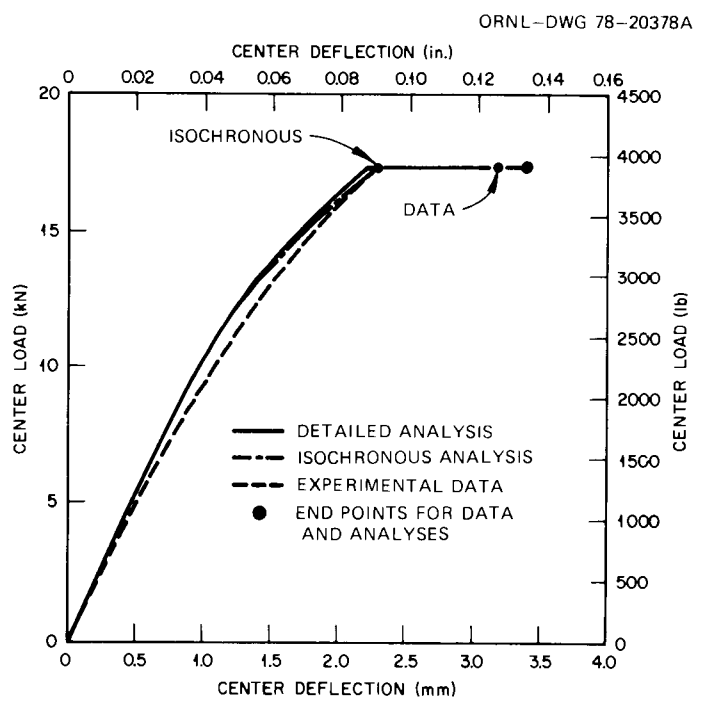

Fig. 20. Comparison among solutions and data in terms of center deflection vs load for plate CP5.

Table 10. Comparison of solutions to test data for beam B9

Method	Histogram point[a]	Error[b] (%) in the solutions	
		Center DCDT	Average strain
Detailed	2	−19.2	+10.2
	3	−5.3	
	Creep (2–3)	+43.8	
Isochronous	2	−19.2	+10.2
	3	−21.3	
	Creep (2–3)	−28.6	

[a]Histogram points are defined in subsection 2.1.

[b]This is relative error (compared to experimental data). A "+" means an overprediction; a "−," an underprediction.

Table 11. Comparison of solutions to test data for plate CP5

Method	Histogram point[a]	Error[b] (%) in the solutions	
		Center DCDT	Average strain
Detailed	2	−7.3	+31.8
	3	+6.3	
	Creep (2–3)	+47.4	
Isochronous	2	−7.3	+31.8
	3	−27.9	
	Creep (2–3)	−90.4	

[a]Histogram points are defined in subsection 2.2.

[b]This is relative error (compared to experimental data). A "+" means an overprediction; a "−," an underprediction.

6.1.3 Observations

The comparisons between detailed solutions and data in Tables 10 and 11 are, taken as a whole, typical for inelastic structural problems such as these two. Small errors in the total deflections (point 3 of histogram) are in these cases the results of cancellations of plastic underpredictions and creep overpredictions; thus, they are believed fortuitously small and should be considered unrepresentative. In both detailed solutions, the errors for the loading segment (point 2 of histogram) and the errors for the creep segment, taken separately, are more in keeping with "typical" errors.

Turning to the comparisons between isochronous solutions and data in Tables 10 and 11, one sees that the magnitude of creep error for the beam was neither unusually large nor small, but for the plate, notably large. Thus, there appears little consistency in the capability of the method to quantitatively predict creep for the two problems considered. Notice also that in both problems isochronous creep predictions were underpredictions while the detailed creep predictions were overpredictions. Though this point seems noteworthy, little explanation concerning the cause can be offered without additional study.

It should also be made clear, since one may be misled by relative error for the two creep solutions for the beam (the isochronous solution error is smaller than the detailed solution error), that the potential for accuracy of the detailed method far exceeds that of the isochronous method. Neither method, however, can be expected to produce exact agreement even for simple beam problems, and in isolated incidences, reversal in the order of agreement (such as occurred for the beam) is not precluded.

6.2 Comparisons Between the Solutions

6.2.1 Comparisons at transducer locations — point comparisons

The solutions at the transducer locations are compared to each other in Table 12. The beam solutions were taken from Tables 6 and 8; the plate

Table 12. Comparison between the two solutions (by the detailed method and by the isochronous method) at the transducer locations

Specimen	Histogram point[a]	Error[b] (%) in the isochronous solution	
		Center DCDT	Average strain
Beam B9	2	0	0
	3	−16.9	−11.2
	Creep (2–3)	−50.3	−34.1
Plate CP5	2	0	0
	3	−32.1	−36.8
	Creep (2–3)	−93.5	−97.5

[a]Histogram points are defined for beam B9 in subsection 2.1 and for plate CP5 in subsection 2.2.

[b]This is a relative error (compared to the detailed solution). The "−" indicates underprediction.

solutions, from Tables 7 and 9. Table 12 records the error in the isochronous solutions assuming the detailed predictions are correct.

Using Table 12 we see that the isochronous method significantly underpredicted the creep deflections and strains in both problems. The plate solution was much worse than the beam solution. Considering the degree of difference between isochronous and detailed solutions for these two structural problems which are relatively simple and of the type for which the isochronous method has straightforward application, one is led to conclude that close correspondence of predictions by the two methods is certainly not guaranteed and may, in fact, be unlikely.

6.2.2 Comparisons using contour plots — whole field comparisons

A comparison between solutions may be accomplished using the contour plots presented earlier as Figs. 7, 8, 13, and 14 (for the beam) and Figs. 9 to 12 and 15 to 18 (for the plate). Comparisons may be made as follows.

Specimen	Component	Comparison: Detailed-to-isochronous	
		Figure number	Figure number
Beam B9	σ_{xx}	7	13
	ε_{xx}	8	14
Plate CP5	σ_{rr}	9	15
	$\sigma_{\theta\theta}$	10	16
	ε_{rr}	11	17
	ε_{zz}	12	18

These comparisons indicate that the detailed and isochronous solutions for total deformations are qualitatively similar. Careful inspection indicates that stresses compare better than strains, which is not surprising since the problems were load-controlled. Also, the two solutions for the beam compare more favorably than the two solutions for the plate. Both beam solutions demonstrate gradual spatial variation of stresses and strains; both plate solutions demonstrate high stress and strain gradients in the plate-to-boss fillet where deformations are heavily concentrated.

It should be noted that the beam solutions were essentially uniaxial in nature everywhere in the beam. In general, the plate solutions were biaxial in nature; in the fillet region all stress components (σ_{rr}, σ_{zz}, $\sigma_{\theta\theta}$, and $\sigma_{r\theta}$) took on appreciable values.

6.2.3 Comparisons at representative cross sections

To provide additional comparisons another method was employed. Transverse "cuts" through the specimens (cross sections) were selected, two each for the beam and plate. Comparisons between the two solutions in terms of average peak values (computed as one-half of the range along the cuts) of the stress and strain components were made. For beam B9, cut 1 was taken on the line of symmetry; cut 2, 5.08 cm (2 in.) away from the line of symmetry. For plate CP5, cut 1 was taken through a section that included the fillets (top and bottom); cut 2, at a distance of 5.61 cm (2.208 in.) away from the center. The comparisons are presented in Table 13. Again, it was assumed that the detailed solution was correct, and the relative error in the isochronous solution was tabulated.

Table 13. Additional comparisons between the two solutions for both beam B9 and plate CP5

Specimen	Cut	Component	Average relative error[a] (%) in the peak values
B9	1	σ_{xx}	−2.6
	1	ε_{xx}	−5.8
	2	σ_{xx}	−2.8
	2	ε_{xx}	−20.1
Plate CP5	1	σ_{rr}	−7.4
	1	$\sigma_{\theta\theta}$	−16.2
	1	σ_{zz}	−10.2
	1	ε_{rr}	−33.3
	1	ε_{zz}	−44.7
	2	σ_{rr}	−12.9
	2	$\sigma_{\theta\theta}$	−4.4
	2	ε_{rr}	−37.5
	2	ε_{zz}	−40.9

[a]The "−" indicates that the isochronous solution was an underprediction.

Considering Table 13, it is seen that the isochronous value was in each case the lesser of the two computed values. For beam B9, stresses were in reasonable agreement at both cuts. Strains were in questionable agreement at cut 2 away from the transverse line of symmetry; the absolute error in ε_{xx} was −0.061% compared to the peak strain value of 0.304% computed by the detailed method.

For plate CP5, the large errors in the stress components at cut 1 were due, in part, to "time-dependent plastic effects"; that is, in the detailed analysis the effective stress $\left(\bar{\sigma} = \sqrt{3/2\ \sigma'_{ij}\sigma'_{ij}}\right)$ at the bottom fillet <u>increased</u> in value from 89 MPa (12.9 ksi) to 95 MPa (13.8 ksi) during the 312-hr hold period, whereas the value due to the isochronous method <u>decreased</u> from 89 MPa to 85 MPa (12.3 ksi) in changing from the 0-hr to the 312-hr isochronous properties. Accompanying the stress increase in the detailed analysis was an increase in the effective plastic strain $\left(\bar{\varepsilon}^p = \sqrt{2/3\varepsilon^p_{ij}\ \varepsilon^p_{ij}}\right)$ from 0.55% to 0.67%. Thus, adding the computed effective creep strain of 0.21%, one determines the sum of the inelastic strains for the detailed solution to be about 0.88%. For the

isochronous solution, however, the sum is only 0.68% (0.55% plastic strain plus 0.13% creep strain).

6.2.4 Observations

The level of solution agreement varies between the two problems. For the case of the beam, the agreement is fairly good; for the plate, poor. One may conclude, though rather tentatively, that the potential for accuracy of the isochronous method is especially problem-dependent. There are significant differences in the beam and plate problems such as the differences in the nature of the stress state and the spatial distribution of deformations. It is suggested that the poor agreement for the plate problem is attributable to the complexity of the stress state and to the extreme inhomogeneity of the deformations produced by the geometry of the plate loading assembly. Beam results support this suggested relationship; for the beam the stress state is essentially uniaxial, the structure uniform, and the agreement between solutions considerably better.

7. SUMMARY AND RECOMMENDATIONS

7.1 Summary

Some capabilities of the inelastic isochronous stress-strain method have been demonstrated through a limited analytical exercise which employed as examples two simple benchmark structural tests. Comparisons among isochronous solutions, detailed solutions, and test data qualified the isochronous predictions of creep deformation and quantified solution accuracy and computing costs.

The study provides information and ideas which should be of benefit to other researchers. It is hoped that the report will complement efforts directed toward devlopment of the isochronous method for utilization in high-temperature structural design.

Some objective statements derived from the study are summarized. The computing costs for isochronous solutions were about 60% cheaper than for detailed solutions for the two problems considered. Also, the isochronous predictions, though they included the gross effects of creep in a qualitatively correct fashion, varied considerably with data and with detailed predictions. The level of agreement varied with the problem; the agreement was better for the beam than for the plate.

7.2 Recommendations

The isochronous stress-strain method has potential for use in design of elevated-temperature structures. However, it is felt that additional activities are needed to identify a specific role for the method to play. It is not clear, for example, whether the method can be validly used (in place of detailed elastic-plastic-creep analysis) to satisfy various ASME Code criteria or, whether it is merely a contrivance with, perhaps, appropriateness of use limited to scoping activities and preliminary design activities.

It is recommended that one follow-on activity be a basic investigation into the underlying theory of the isochronous method. Perhaps such work will identify conditions for appropriate use of the method. Without

such a basic study extraordinary judgment will be required of the designer in modeling with, and in interpreting results provided by this technique.

In the basic investigation it is hoped that answers to the following questions concerning the construction and use of isochronous stress-strain curves will be provided.

1. Is a bilinear isochronous stress-strain curve adequate, or must a nonlinear (or piecewise-linear) curve be employed?
2. What about alterations to the material curve at stresses below yield; should the isochronous stress-strain curves have the same elastic slope as the short-time elastic-plastic curve?
3. How does one construct an isochronous curve to be used in an analysis which involves significant creep but which, in reality, involves no plasticity? Is it more appropriate to perform a nonlinear elastic analysis or an elastic-plastic analysis (both analyses based on the same isochronous stress-strain curve) for such a problem?
4. What are the appropriate yield condition and hardening rule to be used in an elastic-plastic isochronous stress-strain analysis?

Development and validation activities beyond the initial theoretical investigation are also required to answer the following questions.

1. Can the method be adequately extended to treat more general loadings such as step and cyclic loadings, and deformation-controlled loadings involving stress relaxation?
2. Can the method be adequately used in life predictions, and, if so, how?
3. Does the method have the capacity to bound inelastic deformations?

Affirmative answers to all three questions do not constitute a prerequisite for use of the isochronous stress-strain method in design practice;

however, if none can be answered in the affirmative, the uses of the method will certainly be highly limited.

Regardless of the extent of utility of the method in design practice, once the specific role of the method has been determined, it appears necessary to develop and set forth guidelines for application such as has been done for the detailed inelastic method in RDT Standard F9-5T.

8. ACKNOWLEDGMENTS

The author gratefully acknowledges the help, encouragement, and cooperation of several individuals in the planning and preparation of this report. G. T. Yahr provided continuous direction and encouragement to the author; D. T. Godwin aided in the preparation of figures; R. C. Gwaltney, W. K. Sartory, and G. T. Yahr reviewed the manuscript.

9. REFERENCES

1. RDT Standard F9-5T, *Guidelines and Procedures for Design of Nuclear System Components at Elevated Temperature* (September 1974).

2. ASME Code Case 1592-12, "Class I Components in Elevated Temperature Service, Section III, Division 1, ASME Boiler and Pressure Vessel Code, Case Interpretations," The American Society of Mechanical Engineers, New York, September 1977.

3. *High-Temperature Structural Design-1977 Summary and Status Report,* pp. 61–63, ORNL-5419 (July 1978).

4. J. M. Corum, M. Richardson, and J. A. Clinard, *Elevated-Temperature Benchmark Tests of Simply Supported Beams and Circular Plates Subjected to Time-Varying Loadings,* ORNL-5301 (September 1977).

5. J. A. Clinard, *CREEP-PLAST II User's Manual,* ORNL/TM-5868 (May 1978).

6. P. G. Fowler, J. S. Crowell, and J. A. Clinard, *User's Manual for ORNL CREEP-PLAST Graphics Package,* ORNL/TM-4642 (September 1974).

Appendix

USE OF ISOCHRONOUS STRESS-STRAIN METHODS IN PIPING ANALYSIS

There have been a few simplified methods developed for use in inelastic piping analysis. One method developed by Workman and Rodabaugh (and embodied in the piping computer program PIRAX2*) uses flexibility methods to directly account for time-independent elastic-plastic and time-dependent (steady-state) creep behavior of the piping system. Creep (including primary creep) may likewise be introduced, but in a less direct fashion, through the use of isochronous stress-strain techniques.

The PIRAX2 computer program was evaluated by Rodabaugh.† Comparisons were made between test data and PIRAX2 calculations for a problem set which included beam B9. For the creep analysis of beam B9 he used a nonlinear isochronous stress-strain curve and calculated a creep deflection at 312 hr that was 40% higher than the measured creep deflection. Referring to Table 10 herein, one sees that the detailed method overpredicted creep deflection at the center DCDT by a similar margin of 44%, but the isochronous stress-strain method (used in this study) <u>underpredicted</u> creep deflection by 29%.

Several points can be noted concerning these somewhat parallel studies. First, there was a vast difference between the creep deflections predicted for beam B9 using two variations on the isochronous method. Comparing the analytical techniques, we see that Rodabaugh (for his isochronous solution) fit a curve of the form $\varepsilon = A\,\sigma^{n}$ to creep data (elastic and plastic strains not included) and performed a "nonlinear" analysis based on simple beam theory to determine directly the creep deflections. For the analysis reported herein a bilinear isochronous curve (constructed of elastic, plastic, and creep parts) was employed in a two-dimensional finite-element, elastic-plastic analysis; then, creep

---

*G. H. Workman and E. C. Rodabaugh, *User's Manual for PIRAX2, Inelastic Analysis of 3-Dimensional Piping Systems,* ORNL-SUB-3651-3 (December 1974).

†E. C. Rodabaugh, *Evaluations of the Piping System Inelastic Analysis Computer Program PIRAX2,* AI-DOE-13216 (October 1977).

deflection was determined as the difference between total deflections calculated using the 0-hr and 312-hr isochronous curves. It is not surprising that the two differing techniques led to different answers; however, a complete explanation of the large disagreement is not possible without further investigation.

A point is noted that a definite lack of unanimity exists in the two techniques for treating the time-dependent strains, yet both have been labeled "the isochronous stress-strain method."

ORNL/TM-6673
Dist. Category UC-79,
-79h, -79k

INTERNAL DISTRIBUTION

1. B. R. Bass
2. J. J. Blass
3. C. R. Brinkman
4-13. J. A. Clinard
14. C. W. Collins
15. S. J. Chang
16-20. J. M. Corum
21. D. N. Fanning
22. W. H. Gray
23. W. L. Greenstreet
24. R. C. Gwaltney
25. R. L. Huddleston
26. S. K. Iskander
27. W. J. McAfee
28. S. E. Moore
29. T. W. Pickel
30. C. E. Pugh
31. W. K. Sartory
32. J. E. Smith
33. W.C.T. Stoddart
34. R. W. Swindeman
35. G. T. Yahr
36. Patent Office
37-38. Central Research Library
39. Y-12 Document Reference Section
40-48. Laboratory Records Department
49. Laboratory Records (RC)

Subcontractors

50. H. Armen, Jr., Grumman Aerospace Corp., Bethpage, NY 11714
51. C. E. Jaske, Battelle-Columbus Laboratories, Columbus, OH 43201
52. W. J. O'Donnell, O'Donnell and Associates, Pittsburgh, PA 15236
53. D. H. Pai, Foster-Wheeler Energy Corp., Livingston, NJ 07029
54. C. C. Schultz, Babcock and Wilcox Co., P. O. Box 835, Alliance, OH 44601

EXTERNAL DISTRIBUTION

55-56. Director, Division of Reactor Research and Technology, Department of Energy, Washington, D.C. 20545
57. Director, Nuclear Research and Development Division, ORO
58. Assistant Manager, Energy Research and Development, ORO
59-286. Given distribution as shown in TID-4500 under categories UC-79, -79h, -79k